REPORT DOCUMENTATION PAGE

Approved for public release; distribution unlimited.

1. AGENCY USE ONLY (Leave blank)	2. REPORT DATE	3. REPORT TYPE AND DATES COVERED
		FINAL 01 OCT 90 TO 30 SEP 93

4. TITLE AND SUBTITLE

PERFORMANCE METRICS FOR LOW PROBABILITY OF INTERCEPTCOMMUNICATION SYSTEMS (U)

5. FUNDING NUMBERS

2304/A6
AFOSR-91-0018

6. AUTHOR(S)

Professor Glen Prescott

7. PERFORMING ORGANIZATION NAME(S) AND ADDRESS(ES)

University of Delaware
Dept of Mathematical Sciences
Newark, DE 19716

8. PERFORMING ORGANIZATION REPORT NUMBER

AFOSR-TR- 94 0085

9. SPONSORING/MONITORING AGENCY NAME(S) AND ADDRESS(ES)

AFOSR NM
110 DUNCAN AVE, SUITE B115
BOLLING AFB DC 20332-0001

10. SPONSORING/MONITORING AGENCY REPORT NUMBER

AFOSR-91-0018

11. SUPPLEMENTARY NOTES

12a. DISTRIBUTION/AVAILABILITY STATEMENT

APPROVED FOR PUBLIC RELEASE: DISTRIBUTION IS UNLIMITED

12b. DISTRIBUTION CODE

UL

13. ABSTRACT (Maximum 200 words)

The research consisted of two distinct but interrelated problems. First, the researchers performed the research necessary to establish and describe a set of metrics and theorems for Low Probability of Intercept waveforms. This led to the development of a design and analysis methodology and capability for Low Probability of Intercept signals and systems. This methodology and capability resulted in an algorithmic approach to LPI design and is composed of two primary elements - an analytical-based, computer-aided system to evaluate the detectability of LPI waveforms, and computer simulation models which allow the LPI communication link to be simulated and evaluated against the effects of jamming and intercept receivers. Secondly, as these tools were being developed, the researchers conducted basic research into the design of the next generation LPI waveforms and possible strategies for detecting them. The two research tasks were complementary efforts. This research effort had elements of both basic and applied research. The theorems and metrics led to the development of a tool to analyze waveform detectability which will serve two functions. It can be used as a design instrument for the engineer who must select the most effective LPI modulation technique for a given system; and furthermore it can also be used to facilitate basic research in the area of waveform detectability.

14. SUBJECT TERMS

15. NUMBER OF PAGES

16. PRICE CODE

17. SECURITY CLASSIFICATION OF REPORT	18. SECURITY CLASSIFICATION OF THIS PAGE	19. SECURITY CLASSIFICATION OF ABSTRACT	20. LIMITATION OF ABSTRACT
UNCLASSIFIED	UNCLASSIFIED	UNCLASSIFIED	SAR (SAME AS REPORT)

NSN 7540-01-280-5500

Standard Form 298 (Rev. 2-89)

Final Technical Report
to
Air Force Office of Scientific Research
AFOSR/NM (Mathematics & Signal Processing)
Bolling AFB, Washington DC 20332-6448
for
Grant #AFOSR-91-0018

Period of Performance: 10/1/90 – 9/30/93

Performance Metrics for Low Probability of Intercept Communication Systems

Glenn E. Prescott
Principal Investigator
Associate Professor
Department of Electrical & Computer Engineering

October 1993

Telecommunications & Information Sciences Laboratory
Department of Electrical Engineering
2291 Irving Hill Drive Campus West
The University of Kansas
Lawrence Kansas 66045

Final Technical Report
to
Air Force Office of Scientific Research
AFOSR/NM (Mathematics & Signal Processing)
Bolling AFB, Washington DC 20332-6448
for
Grant #AFOSR-91-0018

Period of Performance: 10/1/90 – 9/30/93

Performance Metrics for Low Probability of Intercept Communication Systems

Glenn E. Prescott
Principal Investigator
Associate Professor
Department of Electrical & Computer Engineering

October 1993

Telecommunications & Information Sciences Laboratory
Department of Electrical Engineering
2291 Irving Hill Drive - Campus West
The University of Kansas
Lawrence Kansas 66045

Contents

List of Figures

List of Tables

Chapter 1

Background and Introduction

1.1 Overview of the Research

Modern military communication systems are required to function in a hostile environment containing jammers and intercept receivers. Their success in achieving reliable secure communications depends a great deal on the nature of the transmitted signal used to convey information. Exotic modulation techniques employing spread spectrum (SS) signals are now being used to give the communications receiver an advantage against jammers. This advantage is in the form of a signal processing "gain" due to the coded nature of the spread spectrum waveform. More recently, however, these same spread spectrum modulation techniques are being investigated for their inherent ability to provide covert, Low Probability of Intercept (LPI) features to the transmitted signal which renders the transmitted waveform difficult for an unintended listener (i.e., intercept receiver) to detect. The thrust of the research reported on here focuses on the latter issue - that is, the study of waveform design for reducing detectability; and the related problem of estimating the detectability of these waveforms.

The research consisted of two distinct but interrelated problems. First, we performed the research necessary to establish and describe a set of metrics and theorems for Low Probability of Intercept waveforms. This led to the development of a design and analysis methodology and capability for Low Probability of Intercept signals and systems. This methodology and capability resulted in an algorithmic approach to LPI design and is composed of two

primary elements - an analytical-based, computer-aided system to evaluate the detectability of LPI waveforms, and computer simulation models which allow the LPI communication link to be simulated and evaluated against the effects of jamming and intercept receivers. Secondly, as these tools were being developed, we conducted basic research into the design of the next generation LPI waveforms and possible strategies for detecting them. The two research tasks were complementary efforts.

This research effort had elements of both basic and applied research. The theorems and metrics led to the development of a tool to analyze waveform detectability which will serve two functions. It can be used as a design instrument for the engineer who must select the most effective LPI modulation technique for a given system; and furthermore it can also be used to facilitate basic research in the area of waveform detectability.

1.1.1 Motivation and Purpose

The Information Transmission Division of the Wright Research and Development Center (WRDC/AAAI) is engaged in research leading to the development of the next generation of airborne communication systems. These systems will be designed to exhibit a significant degree of jam protection and covertness. They will employ advanced modulation techniques (spread spectrum), antenna beam and null steering, and adaptive signal processing technologies which will tune the communication system to the operational environment. The requirement for these systems to achieve covert communications has led to the development of a communications concept described generically as Low Probability of Intercept (LPI). The primary purpose of an LPI capability for a communications system is to prevent an unauthorized listener from determining the presence or location of the transmitter, in order to decrease the possibility of both electronic attack (jamming) and physical attack. Therefore, the design of a communication link to have an LPI capability is predicated on the requirement for it to operate in a hostile environment where unauthorized listeners are actively attempting to detect the presence of the communicator's transmission.

In order to effectively implement the next generation LPI communication systems, researchers and engineers will need analysis tools to evaluate the performance of these systems in a hostile environment. The tools in turn require a set of metrics and procedures to determine system performance.

This was one of the thrusts of our research.

These tools need to be applied early in the design cycle in order to provide a positive influence on system performance, effectiveness and cost. We see these analysis tools for LPI communications to be the following:

1. Analytic or mathematical modeling of the communication environment. This approach seeks to express in closed form the performance parameters of the communicators, jammers and interceptors operating within a common radio frequency environment. From a knowledge of these parameters and the operational environment, a link analysis can be performed which will reveal the vulnerability or susceptibility of various types of LPI communication signals and systems to various types of jammers and interceptors. However, due to the complex nature of a hostile RF environment it may be difficult to provide a meaningful accounting of the influence that all the players have on each other. Therefore, simulation may prove to be an effective way to augment this approach.

2. Simulation-based modeling of the communication environment. While analytic modeling is fast and convenient, not all performance parameters can be expressed in closed form, and not all processes within the operational environment are linear. Therefore, after preliminary analysis is completed using techniques described above, computer simulation can be employed to evaluate LPI communication system performance within any scenario. Nonlinear systems, intermodulation products, and other effects which are difficult to model analytically, are usually quite easily simulated. With simulation, the engineer gets to "run" the system and evaluate it within a particular environment before money is spent on hardware. The disadvantage of simulation is, of course, the long processing times often required to achieve meaningful results.

3. Hardware emulation of the communication environment. The use of hardware emulation requires an extensive laboratory facility so that jammers, communicators and interceptors can be effectively evaluated against each other. WRDC currently has such a facility in its Communication System Evaluation Laboratory (CSEL). However, this analysis tool is only useful after a prototype of the LPI communication system is

available, and represents the last stage of analysis before the system design is fixed. The previous analysis techniques will establish a baseline with which the engineer can evaluate the hardware tests. Without this baseline, the engineer will not know how closely the actual performance can be predicted.

The ultimate value of the analytic and simulation-based models is that they can theoretically predict the performance of proposed configurations without requiring the construction of hardware. This gives the designer a capability to pose a particular scenario consisting of an RF environment populated with jammers and interceptors. This environment can then serve as a testbed for evaluation of proposed LPI waveforms and other LPI techniques against a known or suspected enemy capability. Such a capability could potentially save the Air Force millions of dollars in system development costs by providing the acquisition agency the ability to select the most promising techniques early in the design phase.

For the researcher, these models will be particularly valuable as a tool to aid in the development of the next generation LPI waveforms. These waveforms will be considerably more sophisticated than the spread spectrum modulation techniques currently employed. They will need to be essentially featureless, in that the signal will have no distinctive characteristics which identify it to an interceptor as a communication signal. Considerable research remains to be accomplished in this area. The models developed in this research effort will serve as a testbed for the evaluation of these new waveforms against a variety of detection techniques.

1.2 Introduction

Recent emphasis in military communication systems has focused on the vulnerability of communication signals to interception. While in many instances, an anti-jamming capability is an essential feature for military communication systems, there are many situations in which communications covertness is more important. For example, the requirement for covert operation of military aircraft has led to the reduction of aircraft signatures in order to minimize aircraft detectability. One of the most critical aircraft signatures in this environment is its communication signals. Therefore, the emphasis

on reduced aircraft detectability drives the requirement to limit the interceptability of its communication signals. The result is a low probability of intercept (LPI) communication system.

The characteristics of a communication system which is invulnerable to jamming are quite similar to those of an LPI communication system. The one notable difference is in the received signal-to-noise ratio. For an effective anti-jam (AJ) capability, large receiver signal-to-noise ratios and plenty of excess signal margin are desired. LPI communications, on the other hand, requires the minimum received signal-to-noise ratio necessary to provide the minimum level of acceptable performance.

1.2.1 LPI Signal Exploitation

Military RF communication systems must necessarily provide a high level of security against the exploitation of transmitted information by an unintended listener. This exploitation could be as simple as detecting the presence and location of a communications platform, or as complex as extracting the informa- tion contained in a transmitted signal. Nicholson [8] describes four sequential operations that exploitation systems attempt to perform:

1. Cover the signal that is, a receiver is tuned to some or all of the frequency intervals being occupied by the signal when the signal is actually being transmitted.

2. Detect the signal that is, make a decision about whether the power in the intercept bandwidth is a signal plus noise and interference or just noise and interference.

3. Intercept the signal that is, extract features of the signal to deter-mine if it is a signal of interest or not.

4. Exploit the signal that is extract additional signal features as necessary and then demodulate the baseband signal to generate a stream of binary digits.

The probability that an interceptor can exploit an unknown communication signal is defined as $Pr(E)$, which is given as:

$$Pr(E) = Pr(E|I)Pr(I|D)Pr(D|C)Pr(C) \qquad (1.1)$$

where $Pr(E|I)$ is the probability of exploitation given that the signal can be intercepted, $Pr(I|D)$ is the probability of intercepting the signal given that it can be detected, $Pr(D|C)$ is the probability of detecting the signal given that the signal is covered, and $Pr(C)$ is the probability that the signal is covered. Everything that an unintended listener could conceivably want to do with a signal depends critically on having the ability to cover and detect the presence of the signal. Any subsequent actions are dependent upon signal detection.

Military communication system designers have traditionally employed spread spectrum waveforms to achieve covertness in a transmitted signal. These spread spectrum signals, in addition to permitting the use of code division multiple access (CDMA) for efficient bandwidth utilization, also incorporate significant anti-jam (AJ) and low probability of intercept (LPI) characteristics due to their low-level radiated power densities. The term "LPI" is used here as it is in much of the literature (e.g., [3]), although LPI signals are perhaps better described as low probability of detection (LPD) signals. LPI will be used in this report to describe signals which are difficult for an unintended receiver to detect.

The communications receiver in an LPI communication system possesses knowledge of the code which was used at the transmitter to spread the signal, and thus can de-spread the received signal by re-mixing it coherently with the code. This de-spreading operation allows the receiver to filter out a large portion of the noise power present within the spread bandwidth at the receiver front- end. An unintended receiver does not typically have knowledge of this spreading code and must make signal present decisions based solely on the received energy in some frequency band over some period of time. Furthermore, because the unintended receiver lacks the ability to de-spread the signal, it is unable to filter any of the noise power within the spread bandwidth. Receivers which make binary signal present decisions based on energy detection are called radiometric systems (radiometers), and represent the most common detection threat to LPI signals.

The inherent vulnerability of an LPI spread spectrum signal to detection by a particular radiometric system can be quantified in terms of the required carrier signal power to one-sided noise power spectral density ratio C/N_o

required at the front end of the radiometer to achieve a specified probability of detection P_d and probability of false alarm P_{fa} performance level [7]. The LPI communication system designer uses this detectability information to select the spread spectrum modulation type and parameters to yield a signal which is minimally detectable by the most likely detection threat, in this case a particular type of radiometer system.

Analytical models have been developed which map the radiometer performance probabilities to the required front-end C/N_o. In this report we will develop several of the important analytical models for radiometric intercept receivers and use these to evaluate the detectability of LPI communication waveforms. We will also use these models to obtain a performance metric for the LPI communication system.

1.2.2 System Evaluation

In order to evaluate the potential effectiveness of LPI communication systems, a common criteria is needed to aid in assessing the strengths and weaknesses of proposed techniques. Therefore, quality factors have been developed for LPI communication systems to provide a single, unified quantitative technique which allows the system engineer to evaluate LPI effectiveness in the presence of jammers and intercept receivers. We will concentrate on developing system quality factors for a Low Probability of Intercept (LPI) communication systems; and on describing a methodology for employing these quality factors for a variety of scenarios and systems.

The LPI system quality factors derived in this report originate from the system link equations which describe the signal and interference power gains and losses as a function of path losses, antenna gains, modulation type and interference rejection capability for any given scenario. Quality factors are developed for all major components of the LPI system which can provide some advantage to the cooperative transmitter and receiver over the jammer and intercept receiver.

1.2.3 LPI Techniques

An LPI communications capability for military communication systems is provided via an assortment of technologies and techniques. Many of these are briefly described below:

- Power Control: Transmit power is increased until the receiver acknowledges reception. A feedback control link is required to adjust the transmit power to the minimum necessary for reliable communications.

- Beam Pointing: Highly directional antennas are employed at the receiver and transmitter. Automatic tracking is required to maintain the received signal level, but spatial dispersion of the radiated signal energy is restricted.

- Null Steering Antenna: If the receiver's antenna can place a null in the direction of a jammer, then less power will be needed from the friendly transmitter and thus it will be less detectable.

- Low Sidelobe Antenna: Directional antenna radiates small amounts of power in directions other than the desired direction. However, to reduce spatial dispersion of signal energy to an absolute minimum, antenna sidelobes should be suppressed.

- Frequency Control: Automatic selection of operating frequencies or frequency bands. For example, choose one transmit frequency for the near receiver, another transmit frequency for the distant receiver (e.g., 60 GHz which is highly attenuated, and 54 GHz which propagates further). This technique also includes hopping over several bands, such as HF, VHF, UHF, and L band.

- Bandwidth Compression: Applies primarily to voice communications, but represents any technique which reduces the number of bits per second required for any given transmission. This means the receiver will require less signal strength since each bit can be processed longer.

- Spread Spectrum Modulation: Using frequency hopping, phase shifting, time hopping or their combinations to spread the energy over a band of frequencies and reduce the power density. This makes the transmission less detectable.

- Error Correction Coding: Error correcting codes reduce the signal energy required to maintain a specified level of receiver performance. Any technique which trades power for bandwidth can be used to enhance the LPI performance of a communication system.

- Interference Suppression/Excision: The communication receiver employs a filter that can automatically (or adaptively) place a null at the frequency of a jammer. Therefore, less power will be needed from the communication transmitter to maintain a specified receiver performance level.

- Signal Masking: The communications transmitter intentionally transmits at the same frequency as another radiator but with slightly less power. An intercept receiver will detect the stronger signal. However, the communications receiver will have processing gain and be able to detect the weaker transmission while rejecting the stronger one.

When signal exploitation (i.e., recovery of information from the transmitted signal) is required, the intercept receiver will be operating at a disadvantage to the communications receiver. The communications receiver can employ coherent processing on the spreading code, but the intercept receiver must rely on noncoherent processing, which means that the communications receiver needs less signal power to accomplish its primary task than does the interceptor. On the other hand, when signal detection or interception is required, the interceptor has the advantage in that it only needs to determine the presence of the signal (detection) or extract some characteristics or features from the signal (interception). Since information is not being recovered from the signal, then less received signal power is required for the intercept receiver to accomplish its job.

The effect of each of the techniques discussed above can be observed and evaluated by examining a communication system and intercept receiver in an operational environment, as described later.

Chapter 2

LPI Fundamentals

2.1 Introduction

Figure 2.1 depicts a typical LPI scenario, in which a cooperative transmitter and receiver are targeted by jammers, which disrupt the communications receiver, and intercept receivers, which attempt to detect and exploit the transmitted signal.

The objective of any LPI communication system is to conduct information between a transmitter and receiver while minimizing the ability of an unauthorized listener to intercept, classify, or otherwise exploit the transmitted signal. The communication system has a variety of techniques for reducing the probability of intercept: steerable high gain antennas, adaptive transmitter power control, and transmitted waveforms with large time-bandwidth products and noise-like spectra, just to name a few. Likewise, the interceptor has similar technologies, such as steerable, low sidelobe antennas and adaptive filtering.

2.2 LPI Communication Link Analysis

2.2.1 Link Parameters

The communication system is characterized by several performance parameters which are evaluated to determine how well the system performs. For example, the transmitter is characterized by its power, antenna gain, and

DISCLAIMER NOTICE

THIS REPORT IS INCOMPLETE BUT IS THE BEST AVAILABLE COPY FURNISHED TO THE CENTER. THERE ARE MULTIPLE MISSING PAGES. ALL ATTEMPTS TO DATE TO OBTAIN THE MISSING PAGES HAVE BEEN UNSUCCESSFUL.

any jamming signals are spread at the communication receiver during the despreading operation.

The bandwidth expansion factor is roughly the ratio of the chip rate of the pseudorandom bit stream to the bit rate of the information data. This ratio is generally defined as the processing gain:

$$PG = \frac{R_c}{R_b} \approx \frac{W_{SS}}{W_{data}} \tag{3.1}$$

Figure 4.1 shows how energy is distributed in the time-frequency plane for a DS signal.

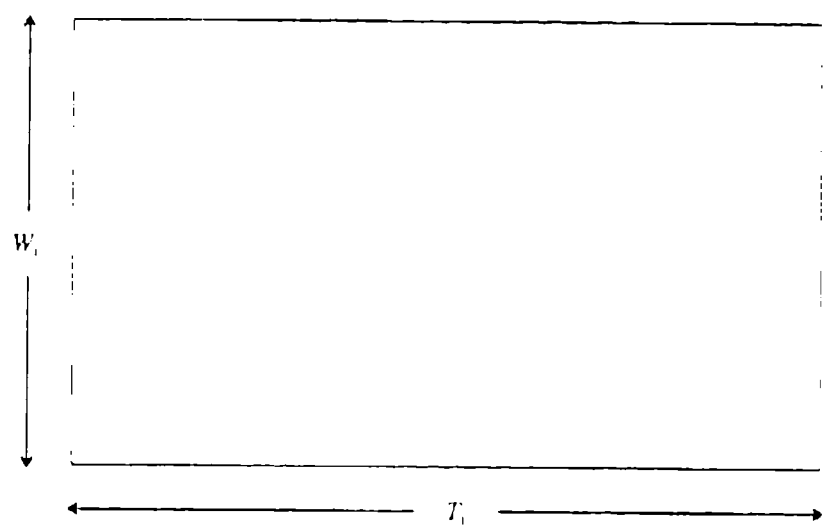

Figure 3.1: Time-Frequency Diagram for a DS BPSK Signal

Because of the spreading, $T_m W_m >> 1$. Assuming the signal is bandlimited to W_m, its energy is measured as follows

$$E = \int_0^{T_m} |s(t)|^2 \, dt \tag{3.2}$$

The energy will be assumed to be constant for all messages of duration T_m.

3.1.2 Frequency-Hopping

Figure 4.2 shows the energy distribution for a frequency-hopped (FH) signal. The total bandwidth and message duration time are W_m and T_m, respectively, while the bandwidth and duration of each hop are W_h and T_h. The value $R_h = 1/T_h$ is called the hop rate. There are M frequency channels (not necessarily contiguous) and N hops in the total message time. LPI (and AJ) capability is achieved by selecting the transmit frequency for each dwell time according to a pseudorandom sequence, known by the intended receiver. Because the interceptor is uncertain which frequency channel is used at any given time, all of the known operating channels must be covered. Since all but one channel contain noise only, the performance of the intercept receiver suffers.

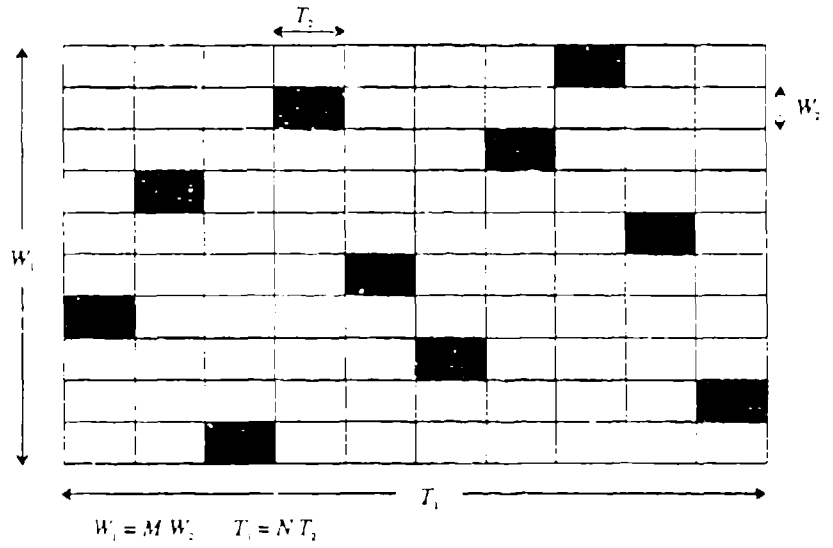

Figure 3.2: Time-Frequency Diagram for a Frequency-Hopped Signal

In a *slow* FH system, the hop dwell time is greater than the data symbol duration (i.e., multiple symbols per hop), and $T_h W_h > 1$. In a *fast* FH system, the hop dwell time is shorter than the symbol duration (multiple hops per symbol), and $W_h \approx R_h = 1/T_h$. In this report, fast frequency

hopping will be assumed.

A pulsed FH signal can be generated by using a duty cycle less than 100 percent. There are no LPI benefits to this modification, however AJ capability can be improved. With pulsed FH, $W_h T_h \approx 1$, but $W_h > R_h$. The duty cycle is given as

$$\alpha = \frac{NT_h}{T_m} \tag{3.3}$$

3.1.3 Time-Hopping

A typical time-hopping (TH) signal is shown in Figure 4.3. This waveform is similar to the FH signal, only pseudorandom time slots of duration are used to transmit the signal instead of frequency channels. During each frame T_F, a time slot T_S is selected, and the total bandwidth W is used. LPI benefits arise because the time uncertainty forces the interceptor to use a longer observation interval than the signal's duration; hence noise-only samples are added to the detection process. Likewise, AJ is improved because the jammer must match its transmission time to that of the communication transmitter. Time-hopping can be combined with the frequency-hopping and direct sequence modulation to further enhance LPI performance.

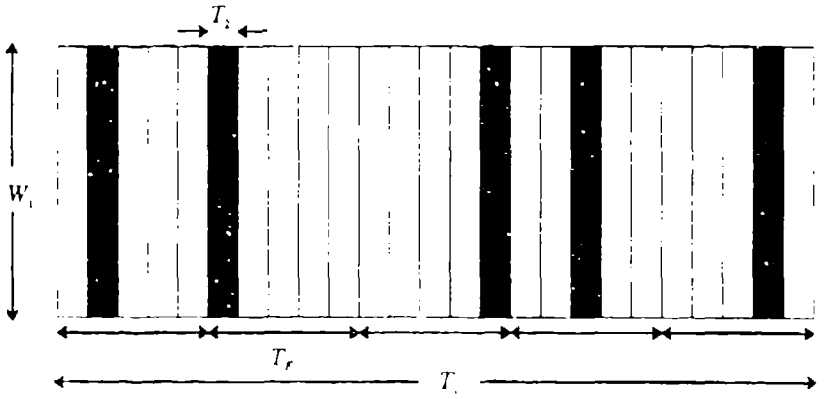

Figure 3.3: Time-Frequency Diagram for Time-Hopped Signal

3.1.4 FH/DS Hybrid

For the pure FH signal, the time-bandwidth product of the individual pulses is nearly unity. LPI capability can be improved by using DS modulation within each pulse, such that $T_h W_h >> 1$. This hybrid gives the advantages of direct-spreading's covertness and the uncertainty of frequency-hopping. An obvious disadvantage is the increased complexity and synchronization requirements.

3.1.5 FH/DS/TH Hybrid

Figure 3.4 shows an example of a signal employing frequency-hopping, direct-sequence spreading, and time-hopping (FH/DS/TH).

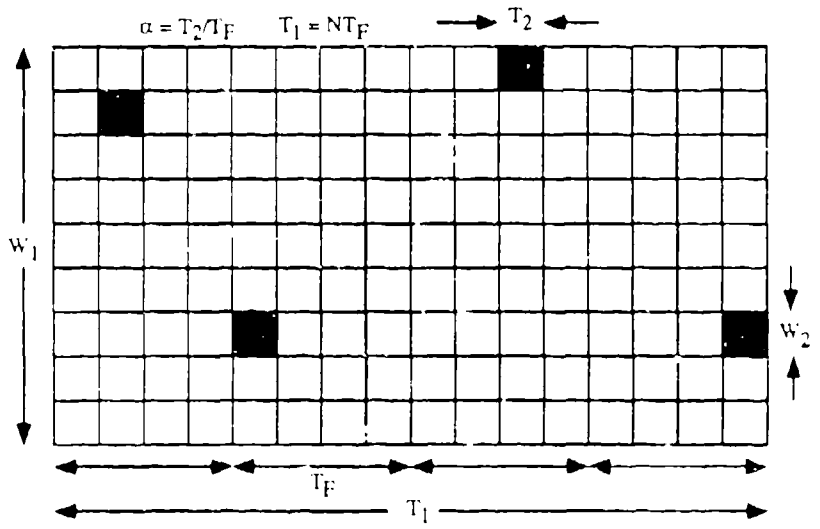

Figure 3.4: Time-Frequency Diagram for FH/DS/TH Signal

As shown in the figure, a message of duration T_m is transmitted using N pulses, each of duration T_h. Each pulse occupies pseudorandomly selected time and frequency slots and has a time-bandwidth product $T_h W_h >> 1$.

The duty cycle of the signal is $\alpha = NT_h/T_m$, giving the signal AJ capability as well.

3.2 A Generic LPI Signal Detection Model

The ability to detect or intercept a spread-spectrum signal depends a great deal on how much the interceptor knows about the signal (i.e., carrier frequency, frequency hop rate, type of digital modulation, etc.). In [11], five levels of interceptor knowledge are defined. At level one, the interceptor knows nothing about the signal, while level five assumes the interceptor has complete knowledge. Neither of the extremes are realistic, and it is generally accepted that the interceptor knows the fixed parameters of the signal and has estimates of the probability distributions of the pseudorandom parameters. This constitutes a "worst case" scenario (from the LPI communicator's perspective), in which the interceptor designs and builds the best possible receiver [6].

R.A. Dillard ([5, 6]) gives a simple detection model, illustrated in Figure 4.5 which can be applied to a variety of scenarios.

Dillard's detection model has two main elements. The *coarse* structure depicts how the data symbols are distributed in time and frequency in the total system time-bandwidth plane. The *micro* structure shows how energy is distributed within each data symbol; the two types of micro structures include pseudonoise (PN) and frequency hop (FH). The individual parameters of the detection model are described in Table 4.1 (from [6]).

In the general, point-to-point LPI scenario, the best intercept receiver often depends on the tranmitted waveform. Sample strategies for the various waveforms are given in [6], [2], and [14], with the common thread being that the detection scheme should be matched to the distribution of energy in the time-frequency space. Generally, the wideband radiometer should be used for DS signals, while the channelized radiometer is better for FH signals and their hybrids.

Such oversimplifications are sometimes false, however, as shown by Engler [2], who shows how the signal parameters (not just the structure) dictate the choice of the intercept receiver to be used. For example, the channelized radiometer is a better detector than the wideband radiometer (i.e., a smaller SNR is required to achieve the same overall P_d and P_{fa}) for mod-

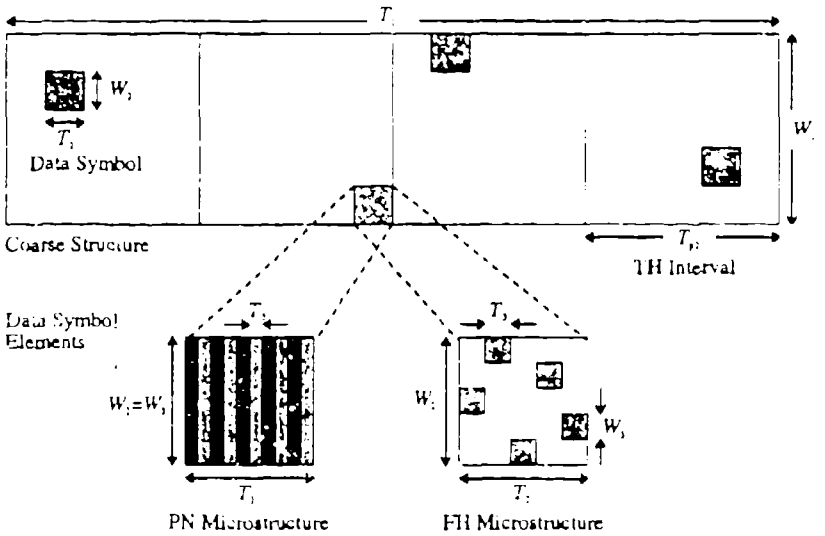

Figure 3.5: Generic Spread-Spectrum Waveform Detection Model

erately small hop rates. However, as the hop rate increases, a threshold is reached beyond which the wideband radiometer performs better, due to the reduced integration times in the channelized detector. This is an important result, because the LPI designer would like to make the wideband radiometer (which provides the least amount of information about the signal) the most effectiveintercept receiver [2, 15].

3.3 Use of LPI Signal Detection Models

A simple detection model for LPI signals (such as suggested in [6]) is often useful in visualizing the complexities of the waveform and providing insight in how to best intercept it. The model employed here describes the frequency bandwidth versus time duration of the transmitted signal. It represents the transmitted waveform as a hierarchy of time-bandwidth units, proceeding from a course structure, which typically has a large degree of complexity (large time-bandwidth product), to progressively finer structures

which eventually approach time-bandwidth products on the order of unity.

A JTIDS-like waveform is chosen as the candidate waveform for the present analysis. The JTIDS detection model employed here is based on the individual time slot (7.8125 msec.). Detection models can also be constructed at higher levels, based on the frame (12 sec.) or the epoch (12.8 min.). The JTIDS -like waveform detection model is illustrated in Figure 3.6. Further details on the JTIDS waveform structure are discussed in [29].

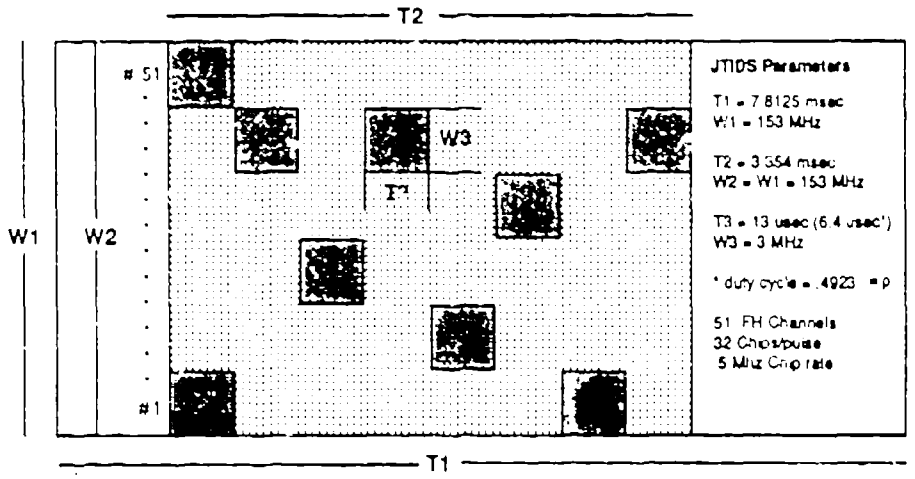

Figure 3.6: Detectability Model for the JTIDS-like Waveform

Note that as the structure of the waveform becomes more fine-grained, additional a priori information is required by the interceptor in order to implement the optimum intercept technique. The performance of the interceptor depends upon how much knowledge the interceptor has about the target signal before an intercept is attempted. Five levels of interceptor a priori knowledge are considered. At level 1 the interceptor has the least knowledge; and at level 5, complete knowledge of the waveform is assumed. In the case of the JTIDS waveform, we can roughly define these levels as follows [11]:

- Level 1 - The interceptor knows nothing about the signal.
- Level 2 - The interceptor has reasonable estimates of T1 and W1, as well as the transmission start and stop times.

- Level 3 - The interceptor knows T1 and W1, and the general time interval structure (as well as start and stop times), and has reasonable estimates on T2.
- Level 4 - The interceptor knows T1, W1, and T2 (as well as start and stop times); and has reasonable estimates on T3 and W3.
- Level 5 - The interceptor knows T1, W1, T2, T3 and W3.

We will assume the interceptor a priori knowledge to be at Level 3 for the analyses that follow.

3.3.1 Nonlinear Intercept Receiver Models

The intercept receiver models considered in this analysis are assumed to perform some nonlinear operation (usually a squaring operation) on the received signal for the purpose of extracting signal energy, or some other waveform feature. We will assume that the interceptor has a priori knowledge at Level 3, but as usual, the spreading codes are unknown. We also assume that the received signal to noise ratio at the intercept receiver is small. This is usually a valid assumption since our LPI quality factor is based on the maximum communication range versus the maximum interception range. At the maximum interception range the signal to noise ratio will be very small. Under these conditions, (and assuming a suitably designed waveform) the optimum receiver has been shown to be a wideband total power radiometer [4]. If feature extraction is the goal of the interceptor, a higher signal to noise ratio is required resulting a smaller intercept range. This causes the LPI quality factor to increase significantly.

For signals having large time-bandwidth products, the output statistics of the radiometer can be assumed to be gaussian, and the detector performance can be completely characterized by the detectability factor δ, which has been defined at the square of the difference in the means of the output densities under noise and signal plus noise conditions [7]. The detectability factor δ, is a measure of the post detection, or output signal-to-noise power ratio of the detector.

$$\delta = [Q^{-1}(P_{fa}) - Q^{-1}(P_d)]^2 = \frac{S_i}{N_{oi} W_2} \tag{3.4}$$

Where W_i is the intercept receiver bandwidth. Five nonlinear radiometer models are assumed for use in the present LPI analysis. These models were suggested for this application in [8].

From these models it is apparent that the total power radiometer requires the least signal power for a successful intercept. Since the total power radiometer is the optimum receiver for detecting the presence of an unknown signal in a gaussian noise environment, we can use it as the standard against which other radiometers and feature detectors are measured.

3.3.2 Communication Receiver Models

For the communications receiver, the performance criterion is the probability of bit error. The probability of bit error can be related to the received $\frac{E_b}{N_{oc}}$ for any particular type of waveform modulation and detection process. This relationship is expressed in the parameter $\zeta_c(P_e)$. Several popular modulation techniques are shown in the table below with the corresponding $\zeta_c(P_e)$:

The JTIDS waveform employs 32-ary orthogonal noncoherent signaling with minimum shift keying as the modulation at the chip level. The expression for the probability of bit error for this modulation technique, which is shown below, is not easily expressed in the form specified for $\zeta_c(P_e)$:

$$P_e = \frac{1}{62}\sum_{n}^{32}(-1)_n\binom{32}{n}\exp[-5\frac{E_b}{N_o}(\frac{n-1}{n})] \tag{3.5}$$

However, the expression can be inverted iteratively, or curves can be used.

3.3.3 Modulation Quality Factor Analysis

An LPI quality factor analysis was performed on a JTIDS -like waveform using the five candidate intercept receivers described in Table 3.2, with the communications receiver operating as described in the previous section, over a wide range of bit error rates. A comparative summary of the modulation quality factor for all five intercept receivers is shown in Figure 3.7. Note that the wideband total power radiometer requires the smallest input signal-to-noise ratio for a successful intercept, as expected.

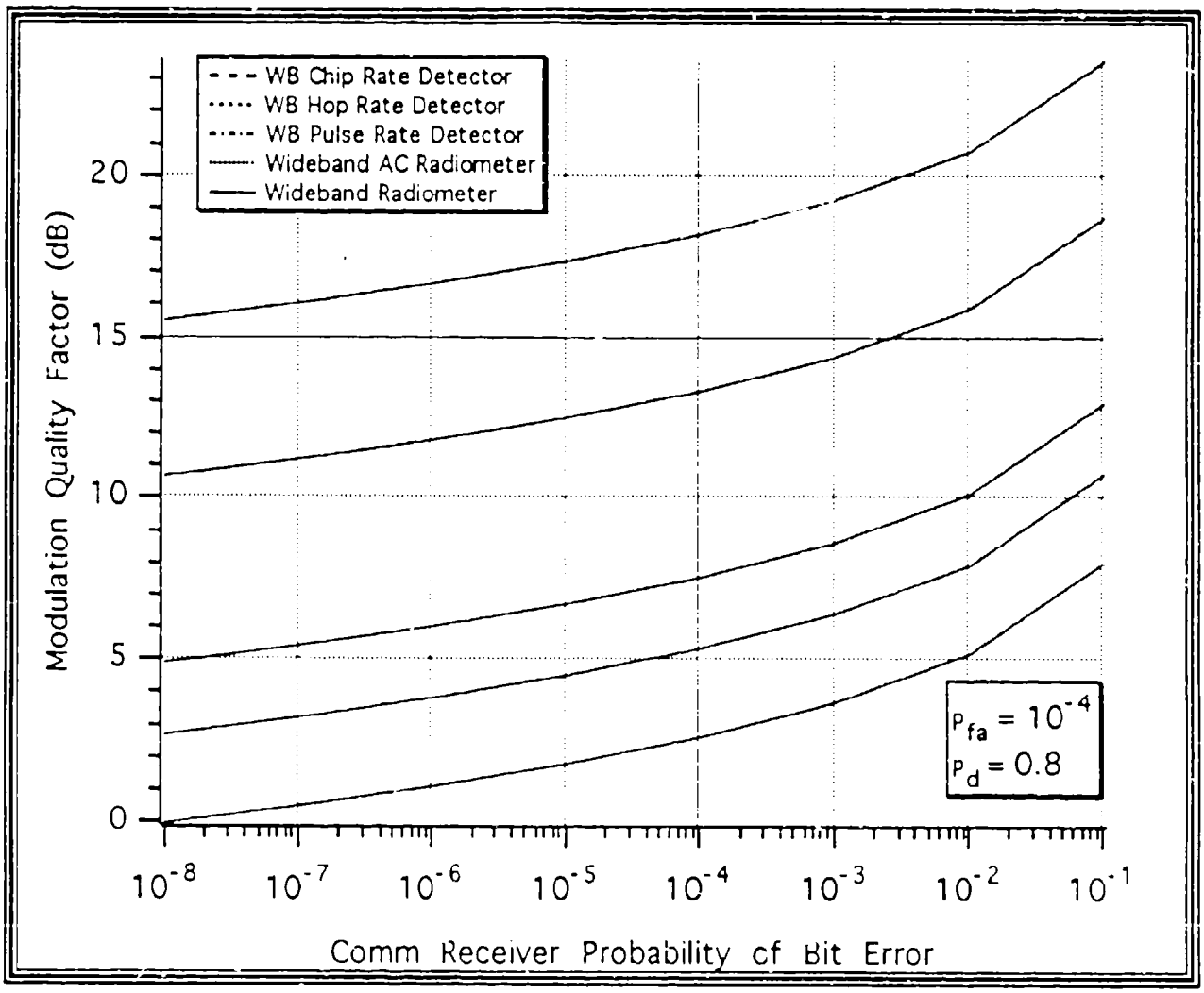

Figure 3.7: Modulation Quality Factors for Nonlinear Intercept Receivers

Signal Structure Categories	*Notation*	*Definition*
All Categories	T_1, W_1	Duration and bandwidth of transmission
	E_1	Signal energy of transmission
Data symbols each contain a number of signaling elements; i.e., the symbol has an FH, TH, or PN structure. If the structure is PN, the value of T_3 usually can be disregarded in detectability calculations.	T_2, W_2	Duration and bandwidth of data symbol
	b_2	Number of data symbols per transmission
	T_{p2}	Duration of hop interval ($T_{p2} = T_1/b_2$)
	E_2	Signal energy in data symbol
	T_3, W_3	Duration and bandwidth of elements ($T_3 W_3 \approx 1$)
	b_3	Number of elements per data symbol
	T_{p3}	Duration of hop interval ($T_{p3} = T_2/b_3$)
	E_3	Signal energy of element
Data symbols each have only one signaling element	T_2, W_2	Duration and bandwidth of data symbol ($T_2 W_2 \approx 1$)
	b_2	Number of data symbols per transmission
	T_{p2}	Duration of hop interval
	E_2	Signal energy of data symbol

Table 3.1: Definitions for Dillard's Signal Detectability Model

Wideband Radiometer Type	$\zeta_1(\mathbf{P_d}, \mathbf{P_{fa}}, \mathbf{T}, \mathbf{W})$
Total Power Radiometer	$\delta\sqrt{\frac{W_1}{T_1}}$
AC Radiometer	$\frac{\delta}{\rho}\sqrt{\frac{2\delta^2 W_1^2}{T_1 T_2}}$
Pulse Rate Detector	$\frac{\delta}{\rho}\sqrt{\frac{2W_1}{T_2}}$
Hop Rate Detector	$\sqrt{\frac{14.36\pi\delta^2 W_1^2}{T_2 T_3 \rho}}$
Chip Rate Detector	$\delta\sqrt{\frac{(318.2)W_1}{T_2}}$

Table 3.2: Intercept Receiver Detection Models

Modulation Type	$\zeta_c(\mathbf{P_e})$
Noncoherent Binary FSK	$-2\ln(2P_e)$
Differentially Coherent Binary PSK	$-\ln(2P_e)$
Coherent Binary & Quadrature PSK	$\frac{1}{2}[Q^{-1}(P_e)]^2$

Table 3.3: Communication Receiver Models

Chapter 4

LPI Signal Detection Models

4.1 LPI Waveforms

As discussed in the previous section, the covertness of a communication link can be improvemed by increasing the modulation quality factor. One way to accomplish this is to select waveforms which are inherently more difficult to detect or intercept. There are many classes of waveforms which can be used for LPI purposes, ranging from simple structures to complex hybrids, and providing different LPI capabilities. Some of these waveforms exhibit antijam (AJ) properties as well.

4.1.1 Direct Sequence Spread Spectrum

Direct sequence (DS) spread spectrum modulation is related to conventional BPSK and QPSK modulation, except a high bit rate pseudorandom binary waveform is combined with the information data stream before modulating the carrier. The result is a waveform having a spectrum many times wider than if just data were used to modulate the carrier. Furthermore, the power spectral density of the waveform is reduced considerably, and is often indistinguishable from background noise.

The communication receiver knows the spreading code used at the transmitter and can despread the signal, in effect yielding a narrowband system. LPI is achieved because the interceptor does not know the spreading code and must therefore use a wideband receiver to capture all of the transmitted energy, thus accepting more noise as well. AJ capability is obtained, because

any jamming signals are spread at the communication receiver during the despreading operation.

The bandwidth expansion factor is roughly the ratio of the chip rate of the pseudorandom bit stream to the bit rate of the information data. This ratio is generally defined as the processing gain:

$$PG = \frac{R_c}{R_b} \approx \frac{W_{SS}}{W_{data}} \tag{4.1}$$

Figure 4.1 shows how energy is distributed in the time-frequency plane for a DS signal.

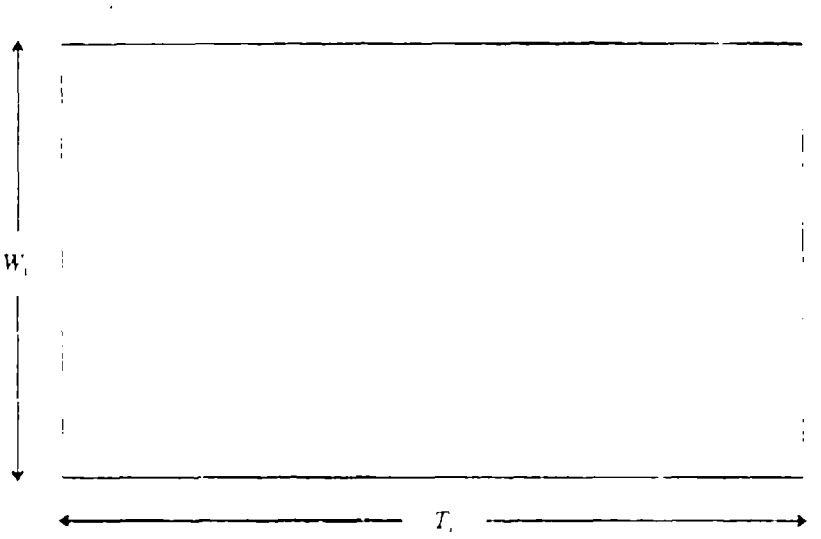

Figure 4.1: Time-Frequency Diagram for a DS BPSK Signal

Because of the spreading, $T_m W_m >> 1$. Assuming the signal is bandlimited to W_m, its energy is measured as follows

$$E = \int_0^{T_m} |s(t)|^2 \, dt \tag{4.2}$$

The energy will be assumed to be constant for all messages of duration T_m.

4.1.2 Frequency-Hopping

Figure 4.2 shows the energy distribution for a frequency-hopped (FH) signal. The total bandwidth and message duration time are W_m and T_m, respectively, while the bandwidth and duration of each hop are W_h and T_h. The value $R_h = 1/T_h$ is called the hop rate. There are M frequency channels (not necessarily contiguous) and N hops in the total message time. LPI (and AJ) capability is achieved by selecting the transmit frequency for each dwell time according to a pseudorandom sequence, known by the intended receiver. Because the interceptor is uncertain which frequency channel is used at any given time, all of the known operating channels must be covered. Since all but one channel contain noise only, the performance of the intercept receiver suffers.

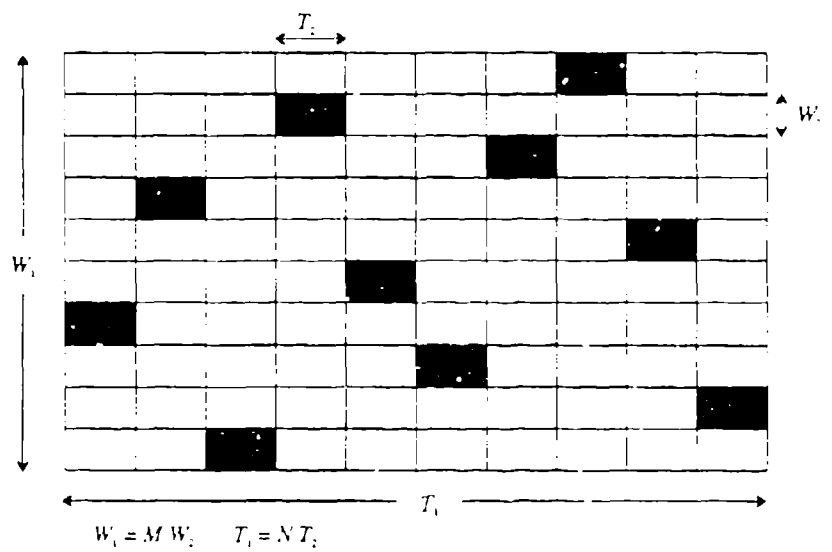

Figure 4.2: Time-Frequency Diagram for a Frequency-Hopped Signal

In a *slow* FH system the hop dwell time is greater than the data symbol duration (i.e., multiple symbols per hop), and $T_h W_h > 1$. In a *fast* FH system, the hop dwell time is shorter than the symbol duration (multiple hops per symbol), and $W_h \approx R_h = 1/T_h$. In this report, fast frequency

hopping will be assumed.

A pulsed FH signal can be generated by using a duty cycle less than 100 percent. There are no LPI benefits to this modification, however AJ capability can be improved. With pulsed FH, $W_h T_h \approx 1$, but $W_h > R_h$. The duty cycle is given as

$$\alpha = \frac{NT_h}{T_m} \tag{4.3}$$

4.1.3 Time-Hopping

A typical time-hopping (TH) signal is shown in Figure 4.3. This waveform is similar to the FH signal, only pseudorandom time slots of duration are used to transmit the signal instead of frequency channels. During each frame T_F, a time slot T_S is selected, and the total bandwidth W is used. LPI benefits arise because the time uncertainty forces the interceptor to use a longer observation interval than the signal's duration; hence noise-only samples are added to the detection process. Likewise, AJ is improved because the jammer must match its transmission time to that of the communication transmitter. Time-hopping can be combined with the frequency-hopping and direct sequence modulation to further enhance LPI performance.

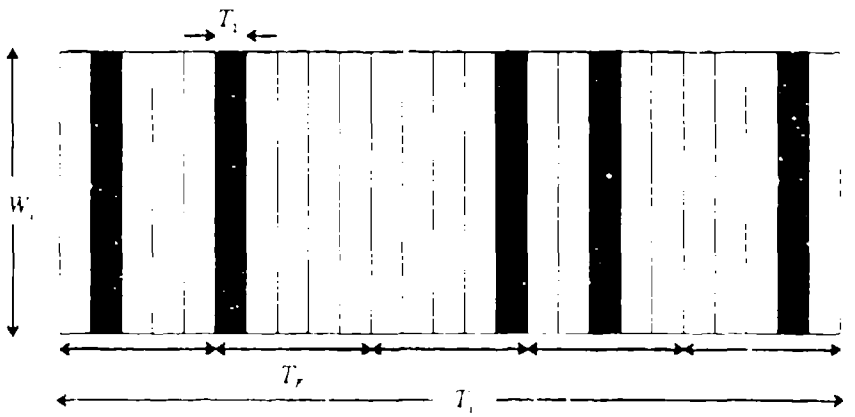

Figure 4.3: Time-Frequency Diagram for Time-Hopped Signal

4.1.4 FH/DS Hybrid

For the pure FH signal, the time-bandwidth product of the individual pulses is nearly unity. LPI capability can be improved by using DS modulation within each pulse, such that $T_h W_h >> 1$. This hybrid gives the advantages of direct-spreading's covertness and the uncertainty of frequency-hopping. An obvious disadvantage is the increased complexity and synchronization requirements.

4.1.5 FH/DS/TH Hybrid

Figure 3.4 shows an example of a signal employing frequency-hopping, direct-sequence spreading, and time-hopping (FH/DS/TH).

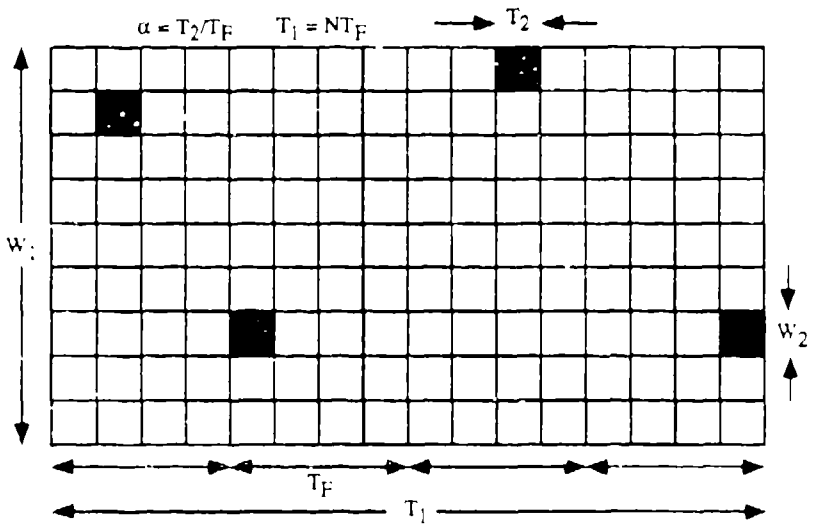

Figure 4.4: Time-Frequency Diagram for FH/DS/TH Signal

As shown in the figure, a message of duration T_m is transmitted using N pulses, each of duration T_h. Each pulse occupies pseudorandomly selected time and frequency slots and has a time-bandwidth product $T_h W_h >> 1$.

The duty cycle of the signal is $\alpha = NT_h/T_n$, giving the signal AJ capability as well.

4.2 A Generic LPI Signal Detection Model

The ability to detect or intercept a spread-spectrum signal depends a great deal on how much the interceptor knows about the signal (i.e., carrier frequency, frequency hop rate, type of digital modulation, etc.). In [11], five levels of interceptor knowledge are defined. At level one, the interceptor knows nothing about the signal, while level five assumes the interceptor has complete knowledge. Neither of the extremes are realistic, and it is generally accepted that the interceptor knows the fixed parameters of the signal and has estimates of the probability distributions of the pseudorandom parameters. This constitutes a "worst case" scenario (from the LPI communicator's perspective), in which the interceptor designs and builds the best possible receiver [6].

R.A. Dillard ([5, 6]) gives a simple detection model, illustrated in Figure 4.5 which can be applied to a variety of scenarios.

Dillard's detection model has two main elements. The *coarse* structure depicts how the data symbols are distributed in time and frequency in the total system time-bandwidth plane. The *micro* structure shows how energy is distributed within each data symbol; the two types of micro structures include pseudonoise (PN) and frequency hop (FH). The individual parameters of the detection model are described in Table 4.1 (from [6]).

In the general, point-to-point LPI scenario, the best intercept receiver often depends on the tranmitted waveform. Sample strategies for the various waveforms are given in [6], [2], and [14], with the common thread being that the detection scheme should be matched to the distribution of energy in the time-frequency space. Generally, the wideband radiometer should be used for DS signals, while the channelized radiometer is better for FH signals and their hybrids.

Such oversimplifications are sometimes false, however, as shown by Engler [2], who shows how the signal parameters (not just the structure) dictate the choice of the intercept receiver to be used. For example, the channelized radiometer is a better detector than the wideband radiometer (i.e., a smaller SNR is required to achieve the same overall P_d and P_{fa}) for mod-

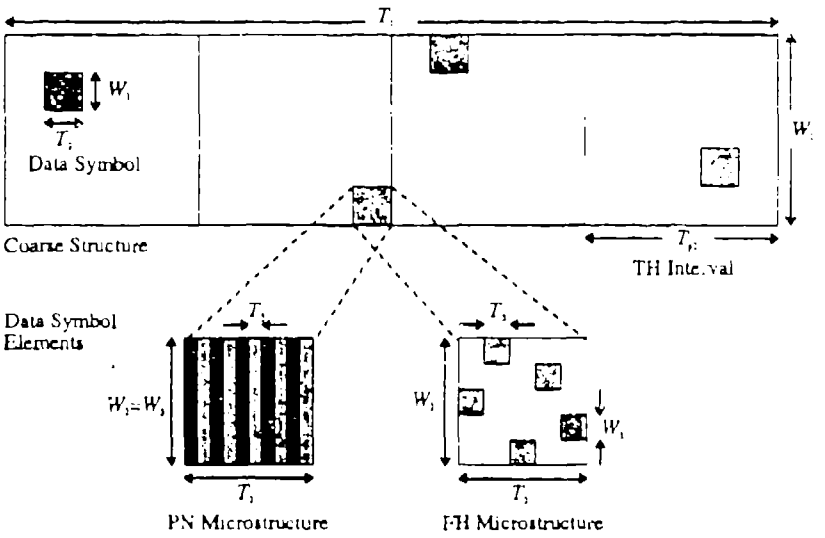

Figure 4.5: Generic Spread-Spectrum Waveform Detection Model

erately small hop rates. However, as the hop rate increases, a threshold is reached beyond which the wideband radiometer performs better, due to the reduced integration times in the channelized detector. This is an important result, because the LPI designer would like to make the wideband radiometer (which provides the least amount of information about the signal) the most effective intercept receiver [2, 15].

Signal Structure Categories	*Notation*	*Definition*
All Categories	T_1, W_1	Duration and bandwidth of transmission
	E_1	Signal energy of transmission
Data symbols each contain a number of signaling elements; i.e., the symbol has an FH, TH, or PN structure. If the structure is PN, the value of T_3 usually can be disregarded in detectability calculations.	T_2, W_2	Duration and bandwidth of data symbol
	b_2	Number of data symbols per transmission
	T_{p2}	Duration of hop interval ($T_{p2} = T_1/b_2$)
	E_2	Signal energy in data symbol
	T_3, W_3	Duration and bandwidth of elements ($T_3 W_3 \approx 1$)
	b_3	Number of elements per data symbol
	T_{p3}	Duration of hop interval ($T_{p3} = T_2/b_3$)
	E_3	Signal energy of element
Data symbols each have only one signaling element	T_2, W_2	Duration and bandwidth of data symbol ($T_2 W_2 \approx 1$)
	b_2	Number of data symbols per transmission
	T_{p2}	Duration of hop interval
	E_2	Signal energy of data symbol

Table 4.1: Definitions for Dillard's Signal Detectability Model

Chapter 5

Radiometer Intercept Receiver Models

5.1 Introduction

In the design of low-probability-of-intercept communication links, the performance of any potential intercept receiver must be considered. The performance of the interceptor is usually specified in terms of its *probability of detection*, P_d, and *probability of false alarm*, P_{fa}, and the required input signal-to-noise ratio (SNR).

The most common intercept receiver is the *wideband radiometer*, which has been discussed extensively in the literature. To simplify the performance analysis of the wideband radiometer, several detectability models have been developed to easily determine the required input SNR for a desired performance level. This paper reviews the development of six such models and compares their results for a variety of performance requirements. When feasible, exact results obtained by numerical integration are also included.

The models to be discussed are those attributed to Torrieri [12], Edell [7], TEAL WING [8, 22], Engler [2], Park [23], and Dillard [6]. There are undoubtedly other models in use, but these are representative and easily found in the literature. Development of the exact solution, which is not solvable in closed form, is also included. Although exact solutions are not difficult to solve using numerical methods, the models are much simpler to use without losing too much accuracy, which will be shown later.

5.2 Model Derivations

Exact Solution

Figure 5.1 shows a block diagram for the wideband radiometer, or energy detector. The detector measures the energy in a bandwidth W Hz over a time interval T sec. If the test statistic V exceeds the detection threshold V_T (determined using one of a variety of criterion, such as Bayes, Minimax, Neyman-Pearson, etc. [24]), the signal of interest is assumed to be present.

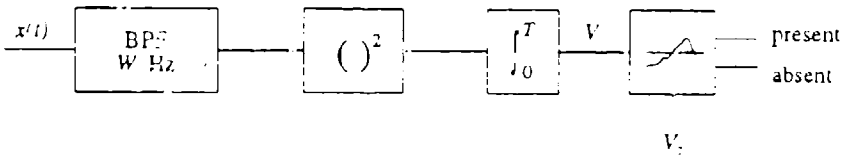

Figure 5.1: Radiometer Block Diagram

It is well known that if the input to the radiometer is strictly additive white Gaussian noise with two-sided power spectral density $N_0/2$, the normalized random variable $Y = 2V/N_0$ has a central chi-square distribution with $\nu = 2TW$ degrees of freedom [12]:

$$p_n(y) = \frac{1}{2^{\nu/2}\Gamma(\frac{\nu}{2})} y^{(\nu-2)/2} e^{-y/2}, \qquad y \geq 0 \tag{5.1}$$

If a signal with energy E (measured over T seconds) is present at the radiometer input, Y has a noncentral chi-square distribution with $2TW$ degrees of freedom and noncentrality parameter $\lambda = 2E/N_0$ [12]:

$$p_{sn}(y) = \frac{1}{2}\left(\frac{y}{\lambda}\right)^{(\nu-2)/4} e^{-(y+\lambda)/4} I_{\frac{(\nu-2)}{2}}\left(\sqrt{y\lambda}\right), \qquad y \geq 0 \tag{5.2}$$

where $I_n(z)$ is the nth order modified Bessel function of the first kind. Equation (5.1) can be obtained from (5.2) by using the series expansion in λ for the Bessel function and letting $\lambda = 0$. Figure 5.2 shows an example of these probability density functions (pdfs) for the case where $TW = 10$ and $\lambda = 20$ ($E/N_0 = 10$ dB). The performance of the radiometer, described in terms of its P_{fa} and P_d, is determined by integrating the conditional density functions

as shown:

$$P_{fa} = \int_{2V_T/N_0}^{\infty} p_n(y)\, dy \tag{5.3}$$

$$P_d = \int_{2V_T/N_0}^{\infty} p_{sn}(y)\, dy \tag{5.4}$$

where V_T is the detection threshold against which V is compared.

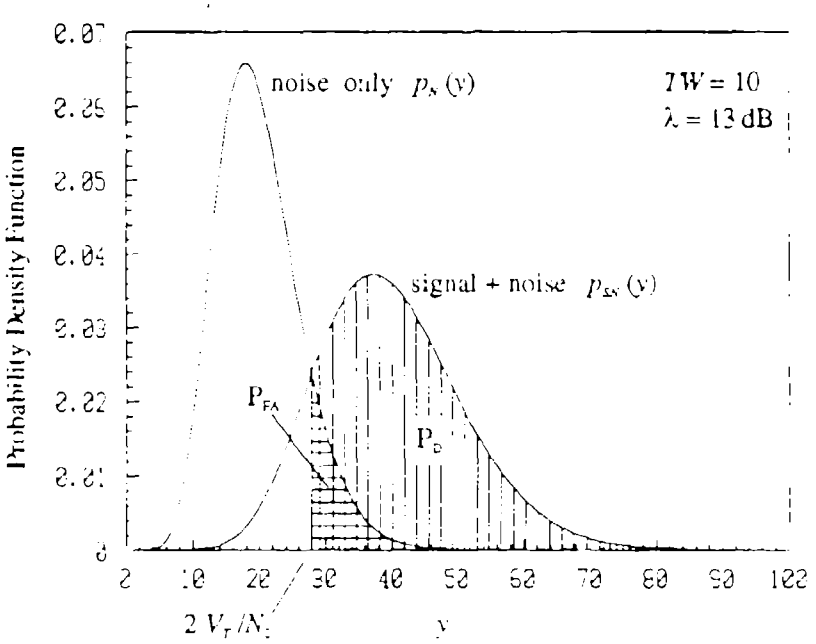

Figure 5.2: Chi-sqare Distributions for $TW = 10$ and $\lambda = 13$ dB

One approach to performance analysis is to determine P_d and P_{fa} for a given signal-to-noise (SNR) ratio and detection threshold. Other approaches would be to determine the required SNR for a desired P_d and P_{fa}, or determine the detection threshold based on an acceptable P_{fa}, and then solve for the P_d given an available SNR. Regardless of the method used, the integrals given in (5.3) and (5.4) are not solvable in closed form and must be evaluated

numerically. Approximations and detection curves based on the numeric results have led to the development of receiver models which yield closed form solutions. These models are discussed in the following sections.

Torrieri's Model

As the number of degrees of freedom becomes large (i.e., the time-bandwidth product is large), the chi-square and noncentral chi-square pdfs asymptotically become Gaussian by the central limit theorem [25]. Torrieri uses this fact in the development of his detection model. His development follows that of Urkowitz [4], in which the signal and noise out of the bandpass filter are broken into their quadrature components. *Sampling theorem* notation is then used to facilitate the analysis, by approximating the integral with discrete summations of the in-phase and quadrature terms. For $TW \gg 1$, the approximations become increasingly accurate. Torrieri shows that for large TW,

$$\mathrm{E}\{V\} = E + N_0 TW \tag{5.5}$$

$$\mathrm{var}\{V\} = 2N_0 E + N_0^2 TW \tag{5.6}$$

Using the Gaussian assumption with no signal ($E = 0$), the false alarm probability is

$$P_{fa} = \frac{1}{\sqrt{2\pi N_0^2 TW}} \int_{V_T}^{\infty} \exp\{-\frac{(v - N_0 TW)^2}{2N_0^2 TW}\}\, dv$$

$$= Q\left(\frac{V_T - N_0 TW}{\sqrt{N_0^2 TW}}\right), \qquad TW \gg 1 \tag{5.7}$$

where $Q(x)$ is the tail integral of the unity variance, zero mean Gaussian pdf,

$$Q(x) = \frac{1}{\sqrt{2\pi}} \int_x^{\infty} e^{-z^2/2} dz = \frac{1}{2}\mathrm{erfc}\left(\frac{x}{\sqrt{2}}\right) \tag{5.8}$$

Since $Q(x)$ is a 1-1 function, it has an inverse (i.e., if $y = Q(x)$ then $x = Q^{-1}(y)$).

If the signal is present and aligned with the radiometer observation interval, then

$$P_d = Q\left(\frac{V_T - N_0 TW - E}{\sqrt{2N_0 E + N_0^2 TW}}\right), \qquad TW \gg 1 \tag{5.9}$$

Solving (5.9) for the E/N_0 required to obtain a specified P_d with a given detection threshold yields

$$\frac{E}{N_0} = 2\xi^2 + \frac{2V_T}{N_0} - 2TW - \xi\sqrt{2\xi^2 + \frac{4V_T}{N_0} - 2TW}, \qquad TW \gg 1 \tag{5.10}$$

where $\xi = Q^{-1}(\sqrt{2}P_d)$. Solving (5.7) for the V_T/N_0 required to obtain the specified P_{fa} and substituting into (5.10) yields

$$\frac{E}{N_0} = \sqrt{2TW}(\beta - \xi) + \psi(\beta, \xi, TW), \qquad TW \gg 1 \tag{5.11}$$

where $\beta = Q^{-1}(\sqrt{2}P_{fa})$ and

$$\psi(\beta, \xi, TW) = 2\xi^2 - \xi\sqrt{2TW}\left[\sqrt{1 + \frac{2\xi^2}{TW} + \frac{8\beta}{\sqrt{2TW}}} - 1\right] \tag{5.12}$$

Finally, the required signal power to noise PSD is obtained using $S = E/T$,

$$\left(\frac{S}{N_0}\right)_{req} = \sqrt{\frac{2W}{T}}(\beta - \xi) + \frac{1}{T}\psi(\beta, \xi, TW), \qquad TW \gg 1 \tag{5.13}$$

Edell's Model

Edell also used the Gaussian assumption to develop a detection model, which is quite simple to use. For $TW > 100$, Edell gives the following for P_{fa} and P_d [7]:

$$P_{fa} = \frac{1}{\sqrt{2\pi}\sigma_n}\int_\gamma^\infty \exp\{-(x-\mu_n)^2/2\sigma_n^2\}\,dx = Q\left(\frac{\gamma - \mu_n}{\sigma_n}\right) \tag{5.14}$$

$$P_d = \frac{1}{\sqrt{2\pi}\sigma_{sn}}\int_\gamma^\infty \exp\{-(x-\mu_{sn})^2/2\sigma_{sn}^2\}\,dx = Q\left(\frac{\gamma - \mu_{sn}}{\sigma_{sn}}\right) \tag{5.15}$$

where $\mu_n = 2TW$, $\sigma_n^2 = 4TW$, $\mu_{sn} = 2TW + 2E/N_0$, and $\sigma_{sn}^2 = 4TW + 8E/N_0$. Note that the detection threshold used by Edell is related to Torrieri's by $\gamma = 2V_T/N_0$. Solving (5.14) and (5.15) for γ and equating yields

$$\gamma = \sigma_n Q^{-1}(P_{fa}) + \mu_n = \sigma_{sn}Q^{-1}(P_d) + \mu_{sn} \tag{5.16}$$

$$Q^{-1}(P_{fa}) - \frac{\sigma_{sn}}{\sigma_n} Q^{-1}(P_d) = \frac{\mu_{sn} - \mu_n}{\sigma_n} \tag{5.17}$$

Edell then used the assumption that $\sigma_{sn} \approx \sigma_n$, implying that the SNR is small and the signal has little effect on the variance of the test statistic. This is generally true when dealing with LPI spread spectrum signals. Using this assumption, we let

$$d = Q^{-1}(P_{fa}) - Q^{-1}(P_d) = \frac{\mu_{sn} - \mu_n}{\sigma_n} \tag{5.18}$$

giving us a relationship between the desired performance and a required SNR, which is the normalized distance between the means of the signal-present and signal-absent probability density functions. The value of d is obtained numerically or from curves given in [7] and in [14]. The term d^2 is often called the *detectability factor*.

Using the values for μ_{sn}, μ_n, and σ_n given earlier, we obtain $d = E/N_0\sqrt{TW}$, or $E/N_0 = d\sqrt{TW}$. Hence, the following well-known detectability model is obtained:

$$\left(\frac{S}{N_0}\right)_{req} = d\sqrt{\frac{W}{T}} \tag{5.19}$$

We will refer to this model as the equal-variance Gaussian assumption (EVGA) model.

For cases where $TW < 100$, the difference between the actual S/N_0 using the exact chi-square statistics and that obtained using the EVGA model can be significant; for example, with $P_d = 0.99$, $P_{fa} = 10^{-12}$, and $TW = 1$, the error is about 7 dB. To account for smaller TW products, Edell includes a correction factor, η, which is defined as follows:

$$\eta = \frac{F(\chi^2, P_d, P_{fa}, T, W)}{G(\text{Gaussian}, P_d, P_{fa}, T, W)} = \frac{F(\chi^2, P_d, P_{fa}, T, W)}{d\sqrt{W/T}}$$

where $F(\chi^2, P_d, P_{fa}, T, W)$ is the predicted S/N_0 using accurate chi-square statistics for the specified P_d, P_{fa}, W, and T, and $G(\text{Gaussian}, P_d, P_{fa}, T, W)$ is the value predicted using the Gaussian assumption. Curves for η are given in [7, 14] for a variety of P_d, P_{fa}, and TW. With the correction factor, Edell's complete model is

$$\left(\frac{S}{N_0}\right)_{req} = \eta d\sqrt{\frac{W}{T}} \tag{5.20}$$

TEAL WING Model

Nicholson [8] presents detection models for several intercept receivers, which were originally developed by Bruce and Snow as part of the 1970s TEAL WING program [22]. As discussed previously, for $TW > 100$, the radiometer test statistic is essentially Gaussian, and the output SNR is related to the input SNR as follows [22]:

$$(SNR)_o = \frac{(SNR)_i^2 TW}{1 + 2(SNR)_i} \tag{5.21}$$

which for small $(SNR)_i$ simplifies to

$$(SNR)_o = (SNR)_i^2 TW \tag{5.22}$$

which is typical of square law receivers with small input SNR. The detectability factor, d^2, is used to relate the required input SNR to the desired performance, as in the case of Edell's model:

$$d^2 = (SNR)_o = (SNR)_i^2 TW \tag{5.23}$$

where d is given in (5.18). Solving for the input SNR yields

$$(SNR)_i = \frac{d}{\sqrt{TW}} \tag{5.24}$$

But $(SNR)_i$ is the ratio of signal power to noise power measured in the intercept bandwidth of the receiver (i.e., $(SNR)_i = S/N_0 W$), so the required signal-to-noise PSD is

$$\left(\frac{S}{N_0}\right)_{req} = d\sqrt{\frac{W}{T}} \tag{5.25}$$

which is identical to the EVGA model.

Engler's Model

Engler's model [2] is based on Barton's detector loss function [26], which permits calculation of the required input SNR to achieve a given P_d and P_{fa} using the detection curves for a coherent receiver with $TW = 1$ (i.e., a single, unmodulated RF pulse). The detector loss function essentially converts a

given amount of SNR, d_I, which is available to a noncoherent receiver to an equivalent SNR, X_0, which provides the same detection performance when applied to a coherent receiver.

The general form of the detector loss function is [2]

$$C(d_I) = \frac{b + d_I}{a d_I} \tag{5.26}$$

which gives the following mapping between d_I and X_0:

$$X_0 = \frac{d_I}{C(d_I)} = \frac{a d_I^2}{b + d_I} \tag{5.27}$$

Because X_0 is the required SNR for coherent receiver performance, (5.27) is easily modified for use with any time-bandwidth product:

$$X_0 = \frac{TW a d_I^2}{b + d_I} \tag{5.28}$$

Barton determined the coefficients a and b in the detector loss function by comparing the noncoherent and coherent detection curves in [24] for a variety of detection requirements. For $TW = 1$, Barton found that $a = 2.0$ and $b = 2.3$ provided the best results. Engler showed that for large TW products ($TW > 10^5$), however, $b = 2.0$ was more accurate, and that the error incurred either way is less than 0.5 dB for all TW products. Solving (5.28) for d_I with $a = b = 2$ yields

$$d_I = \frac{X_0 + \sqrt{X_0^2 + 16TWX_0}}{4TW} \tag{5.29}$$

Engler's d_I is a ratio of signal power to noise power, so we must multiply by the receiver bandwidth to get the required S/N_0:

$$\left(\frac{S}{N_0}\right)_{req} = \frac{X_0 + \sqrt{X_0^2 + 16TWX_0}}{4T} \tag{5.30}$$

The value of X_0 depends on the desired performance (P_d and P_{fa}) and can be obtained from coherent detection curves in [24]. It can also be evaluated numerically as follows:

$$X_0 = \left[Q^{-1}(P_{fa}) - Q^{-1}(P_d)\right]^2 = d^2 \tag{5.31}$$

Park's Model

Park's model [23], also suitable for all ranges of TW, is given as

$$\left(\frac{S}{N_0}\right)_{req} = \zeta d\sqrt{W/T} \tag{5.32}$$

where the correction factor ζ is

$$\zeta = \frac{1}{4}\sqrt{\frac{d^2}{TW}}\left(1+\sqrt{1+18.4\frac{TW}{d^2}}\right) \tag{5.33}$$

Hence, the Park and Edell models are identical in form, except curves for the correction factor are no longer required for small TW products. Park derives his expression for ζ from Barton's detector loss function, using the coefficient $b = 2.3$ in (5.26) instead of $b = 2.0$ as used by Engler. Therefore, it is easy to show that Park's model can also be expressed in Engler's form:

$$\left(\frac{S}{N_0}\right)_{req} = \frac{X_0 + \sqrt{X_0^2 + 18.4TWX_0}}{4T} \tag{5.34}$$

where X_0 is defined in (5.31).

Dillard's Model

Barton's detector loss function allows simple computation of the performance of a noncoherent receiver with any TW product using *coherent* detection curves for $TW = 1$. Urkowitz [27] used Barton's noncoherent integration formulas to show that receiver performance could be determined using *noncoherent* detection curves for $TW = 1$ as well. Using this approach, we can obtain the detection model given by Dillard [5].

Barton defines the noncoherent integration loss as

$$L_n = \frac{D_n}{D_1/n} = \frac{nD_n}{D_1} \tag{5.35}$$

where D_n is the required single sample SNR for a desired P_d and P_{fa} when n samples are noncoherently integrated. Barton also shows that

$$L_n = \frac{C_n}{C_1} = \frac{(D_n + 2.3)D_n}{(D_1 + 2.3)D_1} \tag{5.36}$$

where C_n is the detector loss when the input SNR is D_n (note that the coefficient $b = 2.3$ from Equation (5.26) is used). Equating (5.35) and (5.36) and solving for D_n yields

$$D_n = \frac{D_1^2 + \sqrt{D_1^4 + 9.2nD_1^2(D_1 + 2.3)}}{2n(D_1 + 2.3)} \tag{5.37}$$

Dillard's detection model is then obtained by completing the square in the numerator of (5.37) and using $n = TW$, $\rho = D_1$, and $D_{TW} = S/N_0W$, resulting in

$$\left(\frac{S}{N_0}\right)_{req} = \frac{4.6W}{\sqrt{1 + 9.2TW(\rho + 2.3)/\rho^2} - 1} \tag{5.38}$$

which is Dillard's Equation (2) modified for S/N_0 instead of E/N_0. The value of $\rho = D_1$ can be obtained from single pulse noncoherent radar detection curves or from an analytic approximation given in [24]: [1]

$$\rho \approx \frac{1}{2}\left(\sqrt{-2\ln(P_{fa})} - Q^{-1}(P_d)\right)^2 \tag{5.39}$$

Note that Dillard's model can be modified using 2.0 instead of 2.3 in Equation (5.36), resulting in

$$\left(\frac{S}{N_0}\right)_{req} = \frac{4W}{\sqrt{1 + 8TW(\rho + 2)/\rho^2} - 1} \tag{5.40}$$

which, according to Engler, is more accurate for large TW.

Like Torrieri and Edell, Dillard uses the Gaussian approximations for large TW as well. In fact, Dillard's development proceeds identically to that of Edell. Using the normal approximations provided by Urkowitz [4], Dillard gives

$$P_{fa} = F\left(\frac{2TW - \gamma}{\sqrt{4TW}}\right) \tag{5.41}$$

$$P_d = F\left(\frac{2E/N_0 + 2TW - \gamma}{\sqrt{4TW + 8E/N_0}}\right) \tag{5.42}$$

[1] The SNR values obtained from curves and equations in [24] require adjustment by 3 dB, since DiFranco and Rubin define SNR as $2E/N_0$

where γ is the detection threshold, and

$$F(x) = \frac{1}{\sqrt{2\pi}} \int_{\infty}^{\blacksquare} e^{-z^2/2} dz = 1 - Q(X) \tag{5.43}$$

Note that these equations are equivalent to (5.14) and (5.15). Solving (5.41) for γ and substituting into (5.42) gives

$$P_d \approx F\left(\frac{\frac{E/N_0}{\sqrt{TW}} - F^{-1}(1 - P_{fa})}{\sqrt{1 + (2E/N_0)/TW}} \right) \tag{5.44}$$

which Dillard calls the *full normal approximation*. For $2E/N_0 \ll TW$ (i.e., small SNR), (5.44) can be simplified to

$$P_d \approx F\left(\frac{E/N_0}{\sqrt{TW}} - F^{-1}(1 - P_{fa}) \right) \tag{5.45}$$

which Dillard refers to as the *simple normal approximation*. The simple normal approximation is equivalent to the EVGA model. This is easily verified by solving (5.45) for E/N_0 and using $F(x) = 1 - Q(x)$ and $F^{-1}(y) = Q^{-1}(1 - y)$.

5.3 Model Comparisons

Table 5.1 summarizes the radiometer detection models presented in this paper. As seen in the previous section, they differ primarily in their assumptions and simplifications. Several models are based on the work of Urkowitz, who showed that the conditional probability density functions for the radiometer's test statistic are of the chi-square form, and that they become asymptotically Gaussian as TW becomes large. Other models are based on Barton's detector loss function and signal detection theory. Because of these similarities, we would expect little difference in how they predict the required SNR to achieve some desired performance level.

In Figure 5.3, results from the detection models are compared to exact solutions for a range of TW products, with $P_{fa} = 10^{-6}$ and $P_d = 0.9$. FORTRAN algorithms from the International Mathematical Statistical Libraries (IMSL) [28] were used to evaluate Equations (5.3) and (5.4) to obtain the exact results. The complete Edell model is not shown because of the inherent errors incurred in manually reading correction factors from curves in [7, 14]. For $TW < 1000$, the Dillard (noncoherent integration) and Park models are most accurate, while for $TW > 1000$, the Torrieri and Engler models become more accurate. For $TW > 10^6$, the Torrieri, Engler, and EVGA [2] models converge to the exact results, while the Dillard and Park models give errors of 0.43 and 0.3 dB, respectively.

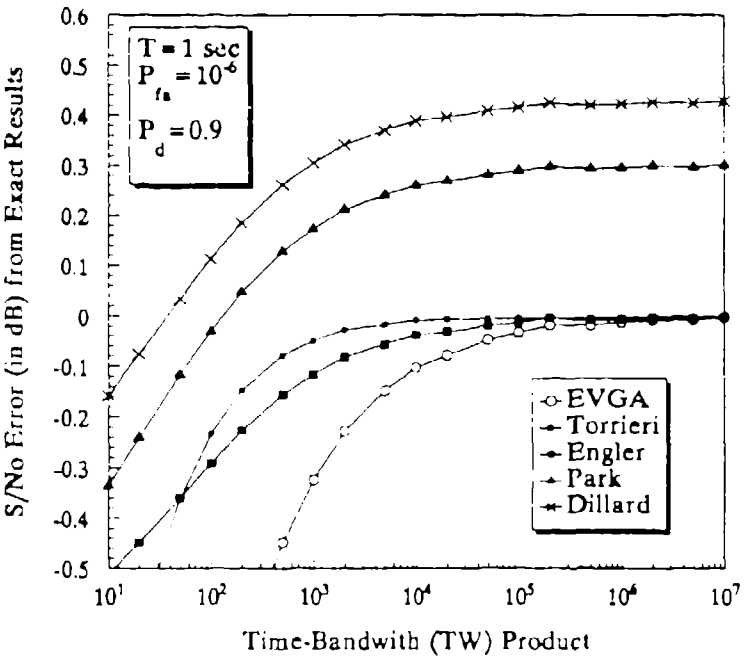

Figure 5.3: Radiometer Model Comparison with Exact Results

Figure 5.4 shows receiver operating characteristic (ROC) curves for $P_{fa} =$

[2] Recall that the EVGA, TEAL WING, and simple normal models are identical, with $S/N_0 = d\sqrt{W/T}$

10^{-6} and $TW = 10$. Again, we see that Dillard's noncoherent integration model is the most accurate for small TW, although all of the models agree within about 0.3 dB of the exact results. The EVGA and Torrieri models were not used since they are not appropriate for small TW.

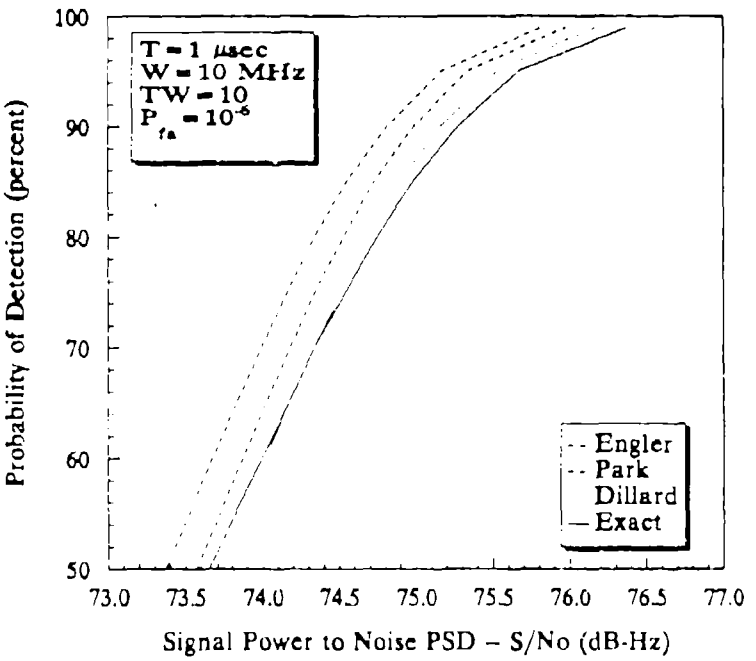

Figure 5.4: Radiometer Model Comparison for $TW = 10$

Figure 5.5 shows ROC curves with $P_{fa} = 10^{-8}$ and $TW = 10^9$. In this case, the Torrieri, EVGA, and Engler models provide the same results, represented by the solid line. The Park and Dillard models differ from the EVGA curve by about 0.3 and 0.4 dB, respectively. Exact results were not calculated for the very large TW case because of limitations in the IMSL software, but from Figure 5.3, it is reasonable to assume that the EVGA model produces nearly exact results.

5.4 Conclusions

Several detection models for the wideband radiometer have been presented in this section. The purpose of these models is to provide a simple means of predicting the required signal-to-noise ratio to achieve some desired performance (P_d and P_{fa}). Comparisons with exact results showed that the Torrieri, Engler, and equal variance Gaussian assumption models converge to the exact results for very large time-bandwidth products. For $TW > 1000$ the maximum error using any of the models is less than 0.5 dB, so all of the models are sufficiently accurate for most purposes.

Torrieri	$(S/N_0)_{req} = \sqrt{\frac{2W}{T}}(\beta - \xi) + \frac{1}{T}\psi(\beta, \xi, TW), \qquad TW > 100$ T = integration time (sec) W = receiver bandwidth (Hz) $\xi = Q^{-1}(\sqrt{2}P_d)$ $\beta = Q^{-1}(\sqrt{2}P_{fa})$ $\psi(\beta, \xi, TW) = 2\xi^2 - \xi\sqrt{2TW}\left[\sqrt{1 + \frac{2\xi^2}{TW} + \frac{8\beta}{\sqrt{2TW}}} - 1\right]$
EVGA TEAL WING simple normal	$(S/N_0)_{req} = d\sqrt{W/T}\ , \qquad TW > 100$ $d = Q^{-1}(P_{fa}) - Q^{-1}(P_d)$
Edell	$(S/N_0)_{req} = \eta d\sqrt{W/T}$ η = correction factor (obtained from curves)
Engler	$(S/N_0)_{req} = \left(X_0 + \sqrt{X_0^2 + 16TWX_0}\right)/4T$
Park	$(S/N_0)_{req} = \left(X_0 + \sqrt{X_0^2 + 18.4TWX_0}\right)/4T$ $X_0 = d^2 = [Q^{-1}(P_{fa}) - Q^{-1}(P_d)]^2$
Dillard	$(S/N_0)_{req} = 4.6W/\left(\sqrt{1 + 9.2TW(\rho + 2.3)/\rho^2} - 1\right)$ $\rho = \frac{1}{2}\left(\sqrt{-2\ln(P_{fa})} - Q^{-1}(P_d)\right)^2$

Table 5.1: Summary of Radiometer Detection Models

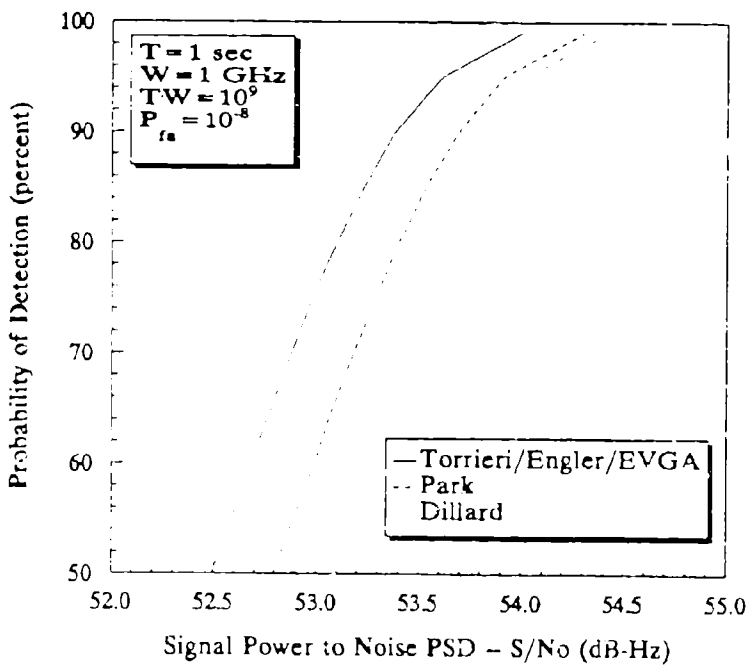

Figure 5.5: Radiometer Model Comparison for $TW = 10^9$

Chapter 6

Post-Processing Detection Models

6.1 Introduction

When detecting frequency-hopped and/or pulsed signals, the interceptor can do either of the following: (1) employ a single wideband radiometer whose bandwidth covers the total spread spectrum bandwidth and integrate over the message duration, or (2) use radiometers matched to the duration and bandwidth of the individual pulses, and then form overall detection decisions based on a variety of procedures for combining the individual pulse detection decisions. The second method, called *double threshold detection*, is generally superior because the time-bandwidth products of the pulses are much smaller than the overall time-bandwidth product of the message, thus reducing the effect of noise on the detection process. This type of detection processing is also known in the literature under the following names [6]: binary integration, "k-out-of-b"detection, and coincidence detection. Several double threshold detectors will be discussed in the following sections.

6.2 Binary Moving Window Detector

A common double threshold detector which is effective against pulsed signals is the binary moving window detector (BMWD), shown in Figure 6.1. The detector forms a soft decision (designated by a "0" or "1") at the end

of each pulse interval. If a sufficient number of pulses have been detected within the last N samples, an overall detection is declared. Dillard's notation for this detector is F-ED-BMW, signifying single-filter energy-detection (i.e., radiometer) followed by binary moving-window detection.

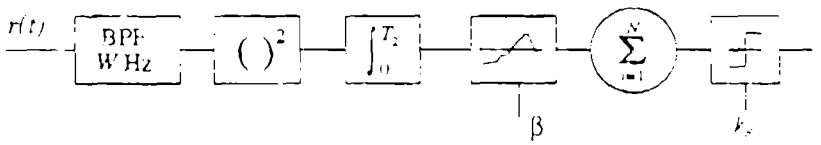

Figure 6.1: Binary Moving Window Detector

As an alternative to using a running sum, the contents of the binary accumulator can be reset following an overall decision after every N pulses. The performance of the *integrate and dump* detector is slightly easier to analyze. It is assumed that the filter in the radiometer has bandwidth equal to that of the input signal, and the integration time equal to the time slot duration. It is also assumed that the noise samples in each time slot are uncorrelated, so the soft decisions are statistically independent. After N slots have been observed, the soft decisions are summed, and an overall detection is declared if the digital threshold k_N is exceeded.

The overall false alarm probability is the probability that k_N or more, out of N total, soft decisions resulted in a detection when no signal is present. Using Q_F as the probability of false alarm for a particular time slot when no signal is present, the probability of having exactly i false alarms is $\binom{N}{i} Q_F^i (1-Q_F)^{N-i}$, so the overall probability of false alarm is the cumulative binomial sum,

$$P_F = \sum_{i=k_N}^{N} \binom{N}{i} Q_F^i (1-Q_F)^{N-i} \tag{6.1}$$

The overall probability of detection P_D is the probability that k_N or more soft decisions resulted in a detection when the signal was in fact present. If the signal is present in each pulse interval (as in frequency hopping), then each soft decision results in a detection or missed detection for that pulse,

and the overall P_D is solved using the cumulative binomial sum:

$$P_D = \sum_{i=k_N}^{N} \binom{N}{i} Q_D^i (1 - Q_D)^{N-i} \tag{6.2}$$

For the given overall P_F and P_D, the soft decision probabilities Q_F and Q_D can be determined by recursively solving (6.1) and (6.2). A suitable radiometer model, such as Engler's, can then be applied to determine the required input SNR in each time slot:

$$\left(\frac{S_I}{N_0}\right)_{req} = \frac{X_0 + \sqrt{X_0^2 + 16 T_2 W_1 X_0}}{4 T_2} \tag{6.3}$$

where $X_0 = (Q^{-1}(Q_F) - Q^{-1}(Q_D))^2$ and $T_2 = T_1/N$.

If the signal uses time hopping, then every time slot will not contain a signal, and the cumulative binomial sum cannot be used to determine the overall probability of detection, as was shown in (6.2). However, it is easily shown that if b is the number of time slots containing signal, then

$$\begin{aligned} P_D &= 1 - \Pr[\text{no detections, given } b \text{ slots have signal}] \\ &= 1 - \Pr[\text{no false alarms in } N - b \text{ slots}] \ \Pr[b \text{ missed detections}] \\ &= 1 - (1 - Q_F)^{N-b} \ (1 - Q_D)^b \end{aligned} \tag{6.4}$$

Solving for Q_D yields

$$Q_D = 1 - \left(\frac{1 - P_D}{(1 - Q_F)^{N-b}}\right)^{1/b} \tag{6.5}$$

An alternative approach to performance analysis would be to determine the overall detection probability given an available SNR, S_A/N_0. Using Dillard's simple normal approximation, the probability that a time slot containing a signal gives a detection is

$$Q_D = Q\left[Q^{-1}(Q_F) - \frac{S_A \ N_0}{\sqrt{W_1 \ T_2}}\right] \tag{6.6}$$

and the overall P_D is solved using (6.2).

Nothing has been said about the value of k_N up to this point. Ideally, k_N should be optimized to minimize the required input SNR for a certain performance level. The optimum value depends on all of the parameters (P_D, P_F, Q_D, Q_F, N, W_1, T_1, etc.). Dillard [6] and Engler [2] have investigated the problem of optimizing k_N, and both found that the curve relating the required SNR to the value of k_N was fairly flat around the optimum value. Dillard found that the optimum value is about $k_N = 0.5b$, where b is the number of samples into the integrator from the signal plus noise condition. Similarly, Engler found that $k_N = 0.6N$ was best for a wide variety of scenarios, which is consistent with Dillard, since $N = b$ for Engler's test case of frequency hop signal detection.

The approach to analyzing the performance of the binary moving window detector is then summarized as follows. First, the intermediate false alarm and detection probabilities, Q_F and Q_D are determined from the overall performance using (6.1) and (6.2). Then the required input SNR is determined using a suitable radiometer detection model, such as Engler, Park, or Dillard. This approach is effective for all of the double threshold detection schemes.

6.3 OR Binary Moving Window Detector

If it is known that the signal is present in just one out of every N_1 time slots (i.e., a TH or FH/TH signal), the binary moving window detector can be modified to improve performance. The resulting detector, denoted as F-ED-OR-BMW, is shown in Figure 6.2. N_1 pulse decisions are logically ORed, with the result applied to the accumulator. Performance is improved, since noise-only samples are deemphasized.

Let p_0 be the probability that a "1" enters the digital integrator when only noise is present in each of the N_1 time slots. Hence,

$$p_0 = 1 - (1 - Q_F)^{N_1} \tag{6.7}$$

Likewise, if p_1 is the probability that a "1" enters the integrator when a signal is present in one of the N_1 slots,

$$p_1 = 1 - (1 - Q_F)^{N_1 - 1}(1 - Q_D) \tag{6.8}$$

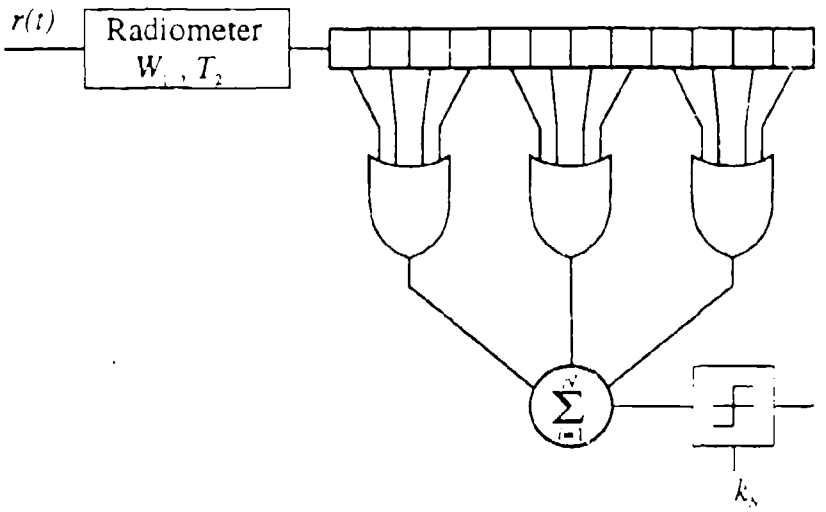

Figure 6.2: Double Threshold Detector with Binary OR Operation

The overall probability of false alarm is simply the cumulative binomial sum,

$$P_F = \sum_{j=1}^{N} \binom{N}{j} p_0^j (1-p_0)^{N-j} \tag{6.9}$$

and if a signal element is present in each of the N trials (i.e., properly synchronized to a time hopping signal), the overall probability of detection is

$$P_D = \sum_{j=1}^{N} \binom{N}{j} p_1^j (1-p_1)^{N-j} \tag{6.10}$$

To determine the input SNR required to obtain the desired P_D and P_F, Equations (6.9) and (6.10) are solved recursively to obtain p_0 and p_1. The time slot performance is then solved using

$$Q_F = 1 - (1-p_0)^{1/N_1} \tag{6.11}$$

$$Q_D = 1 - \frac{1-p_1}{(1-Q_F)^{N_1-1}} \tag{6.12}$$

Engler's radiometer model can then be used with $X_0 = (Q^{-1}(Q_F) - Q^{-1}(Q_D))^2$.

6.4 Filter Bank Detector

If the interceptor knows that the signal occupies a single frequency channel within an overall bandwidth, then improved detection performance can be obtained by channelizing the intercept receiver, as shown in Figure 6.3. The radiometer in each channel integrates over T_1 seconds, with a bandwidth of $W_2 = W_1/M$, where it is assumed that the M channels are contiguous. Although a digital summation and thresholding is shown in the figure, a binary OR operation is generally used, since it is assumed that at most a single channel contains signal (note that the binary OR operation is equivalent to using a digital threshold of $k_M = 1$). Using Dillard's notation, this detector is denoted as FB-ED/OR, signifying filter-bank energy-detection, with OR combining of the soft decisions. The logical OR operation is used because it is assumed that only a single channel contains the signal.

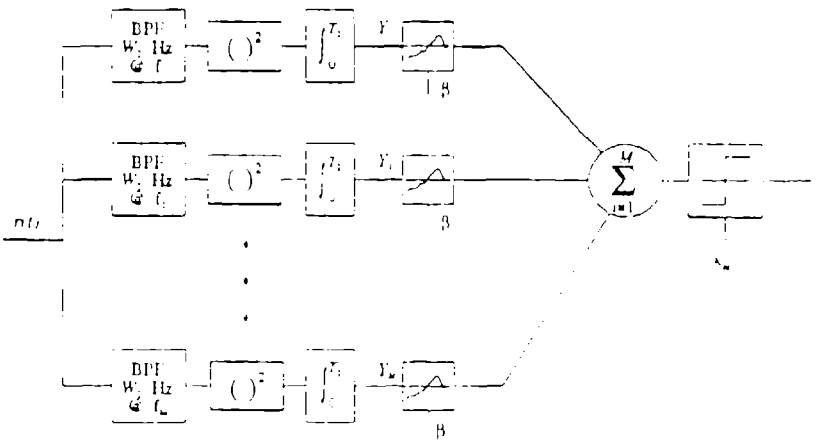

Figure 6.3: Simple Channelized Detector

The overall probability of false alarm, P_F, for the detector is found by computing the false alarm probabilities of each channel. The radiometer bandwidths do not overlap, so the noise processes in the channels are assumed to be statistically independent. It is also assumed that each channel uses the same detection threshold, so the false alarm probability (denoted as Q_F) is

the same for all channels. Therefore the overall probability of false alarm is the probability that one or more channels had a false alarm, even though none had a signal:

$$P_F = \sum_{j=1}^{M} \binom{M}{j} Q_F^j (1 - Q_F)^{M-j} \tag{6.13}$$

Alternatively, P_F can be obtained using the probability that none of the channels has a false alarm,

$$P_F = 1 - (1 - Q_F)^M \tag{6.14}$$

Hence, the single channel false alarm probability is

$$Q_F = 1 - (1 - P_F)^{1/M} \tag{6.15}$$

The overall probability of detection, P_D, is the probability that one or more channels has a detection, given that one of the channels actually contains the signal. If Q_D is the single channel probability of detection, then

$$\begin{aligned} P_D &= 1 - \Pr[\text{no detections}] \\ &= 1 - \Pr[\text{no false alarms in } M-1 \text{ channels}]\ \Pr[\text{one missed detection}] \\ &= 1 - (1 - Q_F)^{M-1}\,(1 - Q_D) \end{aligned} \tag{6.16}$$

Hence, solving for Q_D yields

$$Q_D = 1 - \frac{1 - P_D}{(1 - Q_F)^{M-1}} \tag{6.17}$$

Using Engler's radiometer detection model, the required input SNR to obtain an overall P_F and P_D is computed as follows:

$$\left(\frac{S_I}{N_0}\right)_{req} = \frac{X_0 + \sqrt{X_0^2 + 16T_1W_2X_0}}{4T_1} \tag{6.18}$$

where $X_0 = (Q^{-1}(Q_F) - Q^{-1}(Q_D))^2$, and Q_F and Q_D are solved using (6.15) and (6.17).

6.5 Channelized Radiometer

The FB-ED/OR detector can be modified for detection of frequency hopping signals by matching the filter bank radiometers to the frequency hop times and adding a moving window detector, as shown in Figure 6.4. This receiver is known as a *channelized radiometer*, or *filter bank combiner*, and is denoted as FB-ED-OR/BMW.

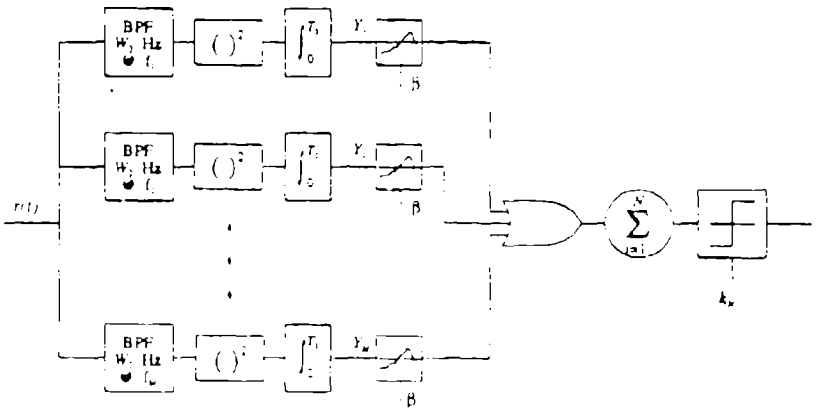

Figure 6.4: Channelized Radiometer (Filter Bank Combiner)

If M contiguous, nonoverlapping channels are used, the bandwidth of each channel is $W_2 = W_1/M$ Hz. For hop dwell times with 100% duty cycle, an integration time of $T_2 = T_1/N$ sec is used. Hence, the total time-frequency space of $T_1 \times W_1$ is partitioned into NM smaller time-frequency cells of size $T_2 \times W_2$. [1]

Usually, the radiometers are identical (same integration time, bandwidth, and detection threshold. After each hop dwell time, each channel makes a detection decision (0 or 1), which is then logically ORed with the other channel outputs, to form a soft decision. The soft decisions are summed over the N hops to form the overall detection decision. It is assumed that

[1] Ideally, the number of channels should be matched to the number of frequencies in the hopset, but fewer channels can be used (for economic and practical reasons) with adequate results [12, 14]

the noise samples in the channels are statistically independent (because their bandwidths are disjoint), and the N soft decisions are independent.

The analysis of the channelized radiometer proceeds quite similarly to the previous detectors. If Q_F is the probability of false alarm for a particular channel radiometer when no signal is present, then the probability that none of the channels has a false alarm is $(1 - Q_F)^M$. Hence the probability of a "1" occuring at the output of the OR gate is

$$p_0 = 1 - (1 - Q_F)^M \tag{6.19}$$

and the probability that this occurs exactly i times is $\binom{N}{i} p_0^i (1 - p_0)^{N-i}$. Hence the overall probability of false alarm is

$$P_F = \sum_{i=k_N}^{N} \binom{N}{i} p_0^i (1 - p_0)^{N-i} \tag{6.20}$$

The overall probability of detection P_D is found similarly. It is assumed that the signal is present during the entire observation interval, $T_1 = NT_2$. If Q_D is the detection probability of a single channel radiometer containing the signal, then the probability of a "1" at the output of the OR gate is found using (6.16):

$$\begin{aligned} p_1 &= 1 - \Pr[\text{no detections in } M \text{ channels}] \\ &= 1 - \Pr[\text{no false alarms in } M-1 \text{ channels}] \Pr[\text{one missed detection}] \\ &= 1 - (1 - Q_F)^{M-1} (1 - Q_D) \end{aligned} \tag{6.21}$$

The overall probability of detection is then obtained using the cumulative binomial sum,

$$P_D = \sum_{i=k_N}^{N} \binom{N}{i} p_1^i (1 - p_1)^{N-i} \tag{6.22}$$

As in the other detectors, it is desirable to solve for the required input SNR for a specified performance level. This is accomplished by solving (6.20) and (6.22) for p_0 and p_1, and then determining the individual channel probabilities Q_F and Q_D:

$$Q_F = 1 - (1 - p_0)^{1/M} \tag{6.23}$$

$$Q_D = 1 - \frac{1 - p_1}{(1 - Q_F)^{M-1}} \tag{6.24}$$

Once Q_F and Q_D have been determined, the required input SNR can be determined using Engler's radiometer model with T_2, W_2, and $X_0 = (Q^{-1}(Q_F) - Q^{-1}(Q_D))^2$.

6.6 Other Detection Schemes

Dillard summarizes several other detection schemes, each especially suited for a particular type of waveform. Calculation of system performance for these schemes proceeds similarly to that presented in the previous section on the channelized radiometer. For LPI detectability calculations, the following procedure is used:

1. Obtain the overall performance (P_D and P_F) of the detector. This is usually dictated by mission requirements.
2. Work backwards using fundamentals of probability theory to determine the required performance levels at intermediate (soft decision) points.

   Solve inverse relationships of any summation operations

   Solve inverse relationships for OR operations
3. Determine the performance requirements (Q_F and Q_D) for the radiometers matched to the individual FH/TH/PN pulses.
4. Use an appropriate radiometer detectability (such as Engler's model) to determine the required SNR to achieve the required Q_F, Q_D.

Bibliography

[1] J.G. Proakis, *Digital Communications*. McGraw-Hill: New York, 1989.

[2] H.F. Engler and D.H. Howard, "A Compendium of Analytic Models for Coherent and Non-Coherent Receivers", AFWAL-TR-85-1118, Georgia Tech Research Institute, September 1985.

[3] P. J. Crepeau, "LPI and AJ Modulation Quality Factors," NRL Memorandum Report 3436, Naval Research Laboratory, Washington D. C., January 1977.

[4] H. Urkowitz, "Energy Detection of Unknown Deterministic Signals", *Proceedings of the IEEE*, vol 55, pp. 523-531, April 1967.

[5] R.A. Dillard, "Detectability of Spread-Spectrum Signals", *IEEE Transactions on Aerospace and Electronic Systems*, vol. AES-15, July 1979.

[6] R.A. Dillard and G.M. Dillard, *Detectability of Spread-Spectrum Signals*, Artech House: Norwood, MA, 1989.

[7] J.D. Edell, "Wideband, Noncoherent, Frequency-Hopped Waveforms and their Hybrids in Low Probability of Intercept Communications", NRL Report 8025, Naval Research Laboratory, 8 Nov 1976.

[8] D.L. Nicholson, *Spread Spectrum Signal Design: LPE and AJ Systems*, Computer Science Press: Rockville, MD, 1988.

[9] R.F. Mills and G.E. Prescott, "A Comparison of Various Radiometer Detection Models", submitted to *IEEE Transactions on Aerospace and Electronic Systems*, May 1993.

[10] L. L. Gutman, and G. E. Prescott, "System Quality Factors for LPI Communications," *Proceedings of the 1989 IEEE International Conference on Systems Engineering*, Dayton, Ohio, August 1989.

[11] E.W. Chandler and G.R. Cooper, "Development and Evaluation of an LPI Figure of Merit for Direct Sequence and Frequency Hop Systems", *Proceedings of the 1985 IEEE Military Communications Conference*, October 1985.

[12] D.J. Torrieri, *Principles of Secure Communication Systems*, Artech House: Norwood, MA, 1992.

[13] Chandler and Cooper MILCOM paper on bandwidth matching for PN SS detection (MILCOM 85)

[14] D. Woodring, D. and J. D. Edell., "Detectability Calculation Techniques", Technical Report SCTN 1977-1, Washington D. C.: Naval Research Laboratory, September 1977.

[15] LPI Waveform Study

[16] Chandler, E. W., and Cooper, G. R. "Low Probability of Intercept Performance Bounds for Spread Spectrum Systems," *IEEE Journal on Selected Areas in Communications*, Vol. SAC-3 No. 5, September 1985.

[17] Polydorus, A. and Weber, C. L. "Detection Performance Considerations for Direct Sequence and Time Hopping LPI Waveforms," *IEEE Journal on Selected Areas in Communications*, Vol. SAC-3, No. 5, September 1985.

[18] Nicholson, David L. "Issues in Signal Design to Lower Probability of Classification and Identification," *Proceedings of the 1987 Military Communications Conference*, Washington, D. C., October 1987.

[19] Nicholson, David L. "Confidence Levels in the Design of Direct Sequence LPE Spread Spectrum Signals," *Proceedings of the 1986 Military Communications Conference*, October 1986.

[20] German, Ed "Optimized, Unstructured Waveforms to Minimize Classification and Identification," *Proceedings of the 1987 Military Communications Conference*, Washington D. C., October 1987.

[21] J. L. Lansford, J. E. Schroeder, and J. E. Hershey, "Use of Markov Chains for Spectral Shaping," *Proceedings of the 1987 Military Communications Conference*, Washington D. C., October 1987.

[22] Bruce, J.D., and K.D. Snow, "Final Technical Report TEAL WING Program," Probe Systems Report PSI-ER327, Probe Systems, Inc., Sunnyvale, Calif., October 1974.

[23] Park, K.Y., "Performance Evaluation of Energy Detector," *IEEE Transactions on Aerospace and Electronic Systems*, vol AES-14, March 1978.

[24] DiFranco, J.V., and W.L. Rubin, *Radar Detection*, Artech House: Dedham, Mass, 1980.

[25] Abramowitz, M., and I.E. Stegun, *Handbook of Mathematical Functions with Formulas, Graphs, and Mathematical Tables*, U.S. Department of Commerce, June 1964.

[26] Barton, D.K., "Simple Procedures for Radar Detection Calculations," *IEEE Transactions on Aerospace and Electronic Systems*, vol AES-5, September 1969.

[27] Urkowitz, H., "Closed-Form Expressions for Noncoherent Radar Integration Gain and Collapsing Loss," *IEEE Transactions on Aerospace and Electronic Systems*, vol AES-9, September 1973.

[28] International Mathematical Statistical Libraries (IMSL), Houston TX, 1991.

[29] TDMA JTIDS Overview Description, Mitre Corporation, MTR8413.

[30] Wright, Robert A., "JTIDS Detectability," Unisys internal technical report Unisys Defense Systems, Communications Systems Division, Salt Lake City, UT.

[31] Robert A Wright, "LPD Analysis of TDMA, Direct Sequence Spread Spectrum Signaling," Internal Memorandum, Paramax Systems Corp, Salt Lake City, UT, March 1992.

Low Probability of Intercept Signal Detectability Analysis (LPI/SDA)

Scott Francis

User's Manual (Version 1.4)

The LPI/SDA User's Manual is included as an adjunct to the final report to describe the implementation of the analytical models. The software described here is available from Prof. Glenn Prescott at the Telecommunications and Information Sciences Laboratory, 2291 Irving Hill Drive, Nichols Hall, University of Kansas, Lawrence, KS, 66045.

Contents

List of Figures

1 Introduction

LPI/SDA, the LPI Signal Detectability Analysis program, is an analytic software tool for the evaluation of the detectability of spread spectrum signals by radiometric detectors and feature detectors. The detectability of a signal is expressed in terms of the signal carrier power to one-sided noise power spectral density required at the front end of an intercept receiver to achieve the user-specified detection and false alarm probability performance. In addition, *LPI/SDA* evaluates five different "Quality Factors" which describe the detectability of a signal separately in terms of scenario-dependent and scenario-independent factors. *LPI/SDA* has the ability to plot one of these Quality Factors, the Modulation Quality Factor, against one of an entire family of parameters which determine its value.

LPI/SDA contains a simple hierarchical user interface which allows the user to specify the type and parameters of the spread spectrum signal, the type and parameters of the radiometer and, if desired, the type and parameters of the feature detector. Range checking is performed on all input parameters, which the user may specify in standard or scientific notation. *LPI/SDA* ensures that the selected signal type and intercept receiver types are compatible.

The user of *LPI/SDA* should be familiar with spread spectrum signals, basic radiometer theory, and general communications theory. A familiarity with *Detectability of Spread-Spectrum Signals* by George and Robin Dillard [1] would be helpful, but the essential items from this source are reviewed in section 2, subsections 1–3.

LPI/SDA can be executed on any 80286- or 80386-based computer with a CGA, EGA, or VGA video adaptor card. If a math coprocessor is present, *LPI/SDA* will use it, otherwise it will emulate it. To run *LPI/SDA*, simply copy the file called LPISDA.exe from the floppy disk to the hard disk, and type `LPISDA`. *LPI/SDA* will prompt you with a menu describing what you may do next. Although *LPI/SDA* does not currently contain on-line help, the actions you may take during an *LPI/SDA* session are presented in the form of both menus and on- screen prompts. Further, *LPI/SDA* ignores spurious input (e.g. typing a character when a numeric is expected) and does dynamic range checking on all input data, so it is unlikely that you will get "stuck" while using *LPI/SDA*.

LPI/SDA was developed by Lawrence Applied Research Corporation in Lawrence, Kansas. Questions pertaining to *LPI/SDA* should be directed to Scott Francis (913) 864-7761, or Glenn Prescott (913) 864-7760. If you discover errors within *LPI/SDA*, please note as thoroughly as possible the actions and input parameters which led to the error and let us know. We will fix the error and send you a revised version of *LPI/SDA* along with our genuine gratitude.

2 Low Probability of Intercept Systems Overview

The following summarizes some of the ideas and notation used in the Dillard text [1], which are also used in *LPI/SDA*. If you are already familiar with chapters 1 and 2 of [1], then you

may wish to proceed directly to section 3, Operating Procedures.

2.1 *LPI/SDA* Signal Notation

LPI/SDA models three regular and four hybrid types of spread spectrum signals. They are:

- Direct Sequence (DS) - also known as pseudonoise (PN)
- Frequency Hopped (FH)
- Time Hopped (TH)
- Frequency Hopped/Direct Sequence (FH/DS)
- Time Hopped/Direct Sequence (TH/DS)
- Frequency Hopped/Time Hopped (FH/TH)
- Frequency Hopped/Time Hopped/Direct Sequence (FH/TH/DS)

From an energy detection standpoint, spread-spectrum signals can be described in terms of relatively few parameters. These parameters are listed below and shown graphically in Figure 1.

- T_1, - message duration (sec)
- W_1 - spread-spectrum bandwidth (Hz)
- T_2 - pulse duration (sec)
- b_2 - number of pulses in T_1
- T_{p2} - hop time duration (sec)
- N - number of frequency hop bands in W_1

These parameters may or may not all be unique. For a hybrid frequency hopped/time hopped/direct sequence signal, for instance, they are all unique. For a direct sequence signal, however, they are not: the pulse duration T_2 is equal to the message time T_1. *LPI/SDA* prompts the user for only those signal parameters which are necessary to describe the signal so that the user is not required to enter redundant parameters.

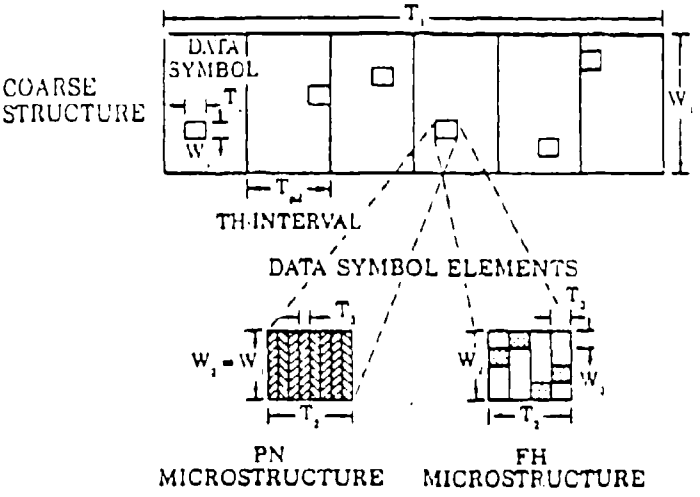

Figure 1: An illustration of signal parameter notation (FH/TH course structure and DS or FH data symbol structure). Adapted from [1].

2.2 Basic Radiometer Theory

The heart of all of the radiometric systems which *LPI/SDA* models is the wideband radiometer (also known as an energy detector or total power radiometer). This system, shown in Figure 2, filters a portion of the RF spectrum, squares this filtered signal to obtain signal power, and integrates from $t-T$ to t to yield signal energy (typically this integration is implemented as integrate and dump rather than continuous integration). This signal energy is then compared to a threshold and, if the threshold is exceeded, a signal is declared present; otherwise no signal is declared present. Assuming ideal signals and filters, the wideband radiometer can equivalently be described as a system which observes a rectangular time-frequency "cell" with bandwidth equal to the bandpass filter bandwidth and time interval equal to the integration time. It measures the total signal plus noise energy received in that cell, and compares this received energy to a threshold. A signal is declared present if the cell energy exceeds the threshold. The performance of the wideband radiometer is characterized in terms of two probabilities: the probability of detection and the probability of false alarm. The probability of detection is defined as the probability that a signal coincides with at least a portion of the radiometer bandwidth, during at least some of the radiometer integration time, and the radiometer declares a signal present. The probability of false alarm is defined as the probability that no signal coincides with the radiometer bandwidth during the integration time, and the radiometer nonetheless declares a signal present.

Intercept receivers which use energy detection can be broadly classified into three categories:

- *Single Filter Energy Detection (SFED)* - These systems observe either the entire spread spectrum bandwidth or one frequency band of a frequency hopped signal. They

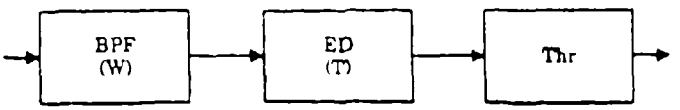

Figure 2: The F-ED-T system (bandpass filter, energy detector, and thresholder). [1]

are typically used against direct sequence, time hopped, or time hopped/direct sequence signals; however they can be used against any type of spread spectrum signal.

- *Filter Bank Energy Detection (FBED)* – These systems utilize a bank of SFED systems, each observing one frequency band of a frequency hopped signal. They are typically used against frequency hopped, frequency hopped/direct sequence, frequency hopped/time hopped, and frequency hopped/time hopped/direct sequence signals.
- *Frequency Scanning Energy Detection (FSED)* – These systems are a more practical approach to very wideband signal detection than the filter bank systems, which often require a prohibitively large number of single filter detectors. The scanning detectors operate by continuously changing the center frequency of the bandpass filter, thereby periodically covering the entire spread spectrum bandwidth. The sensitivity of FSED systems is, as one might expect, a bit less than the sensitivity of FBED systems.

2.3 Radiometric Systems

The following sections describe in greater detail the specific radiometer models contained in *LPI/SDA*.

2.3.1 F-ED-T

The Single Filter–Energy Detect–Threshold radiometer is simply the wideband radiometer described previously. It is the optimum detector for spread-spectrum signals in additive white gaussian noise (AWGN), in the case that the interceptor has no knowledge about the signal except its bandwidth and start time. This radiometer may be used against any type of spread spectrum signal.

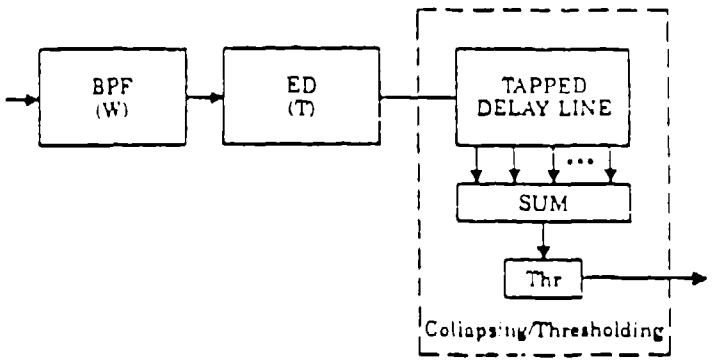

Figure 3: The F-ED-C/T system. [1]

2.3.2 F-ED-C/T

The interceptor can improve his detection performance against time hopped signals if he has knowledge of the positioning of the individual signal pulses in a transmission. This is the function of the Single Filter- Energy Detect-Collapse/Threshold radiometer, illustrated in Figure 3. The total energy in each pulse is determined and inserted into a tapped delay-line. Ideally, the total delay of the tapped delay line should be equal to the message time. The pulse energies in the tapped delay line are summed at the end of the message and compared to a threshold as before. The advantage of using a F-ED-C/T radiometer for time hopped signals lies in the fact that it integrates minimum noise energy since it avoids time intervals in which no signal is present. Further, although it may be unlikely that an interceptor has knowledge of the positioning of the signal pulses of a time hopped waveform which was generated using a pseudorandom code, the time collapsing function could be highly effective against pulsed radar signals which typically have fixed pulse repetition frequencies.

2.3.3 F-ED-BMW

For a hopped signal, an interceptor typically has to make a decision concerning whether he would do better to integrate over the entire transmission, or to integrate over each pulse individually. Further, if he chooses to integrate over each pulse, he must decide whether further processing in his alarm circuit will increase his detection performance [1]. This additional processing is the function of the binary moving-window detector of the Single Filter- Energy Detect-Binary Moving Window radiometer, illustrated

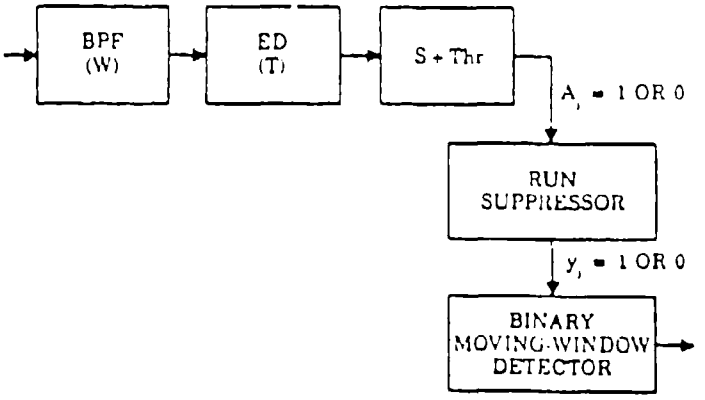

Figure 4: The F-ED-BMW system. [1]

in Figure 4. Every T seconds the output of the sample-and-threshold unit is a 0 or a 1. The run suppressor is used so that a pulse will only contribute a single 1 even if the integration time is not synchronized to the pulse time. The output of the run suppressor is inserted into the binary moving-window detector which, at the end of the transmission, counts the number of pulse detections. If this number exceeds a specified (positive integer) threshold, a signal is declared present. A binary moving-window detector can significantly reduce the false alarm rate by sacrificing a small amount of detection probability.

2.3.4 F-ED-OR/BMW

The Single Filter–Energy Detect–OR/Binary Moving Window radiometer is a slight variation on the F-ED- BMW system. Whereas the F-ED-BMW radiometer assumed knowledge of the pulse position in each hop interval, the F- ED-OR/BMW radiometer assumes knowledge only of the pulse length and the timing of the time hop intervals. In other words, this system knows when pulses *could* occur in each hop interval, but not when they *will* occur. Using this information, and the knowledge that only one pulse can occur per interval, this system matches its integration time to the pulse duration and makes a binary pulse-present decision after each pulse time. This decision is inserted into a binary shift register with length equal to the number of pulse durations per hop interval. At the end of a hop interval, the F-ED-OR/BMW systems performs an OR function over the binary data in the shift register and inserts a 1 into the binary moving-window if at least one pulse detection occurred, otherwise it inserts a 0. The binary moving-window detector makes a signal present decision at the end of

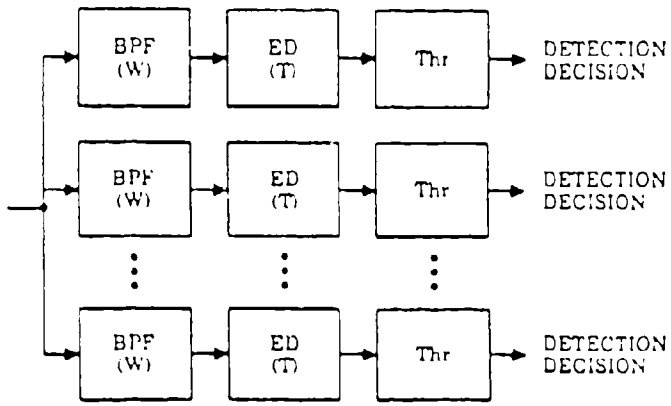

Figure 5: The FB-ED-T system. [1]

the transmission in the same manner as before.

2.3.5 F-ED-OPT

The Single Filter–Energy Detect–Optimum radiometer has decision logic based on a likelihood ratio, which is the optimum detection procedure. See [1] for additional information concerning this system.

2.3.6 FB-ED-T

The Filter Bank–Energy Detect–Threshold system, illustrated in Figure 5, is simply a bank of F-ED-T systems. It is typically used against any type of frequency hopped signal, as are all of the filter bank radiometers, and simultaneous signal detections in multiple frequency bands are treated as one detection. If the number of frequency hop bands is large, the interceptor may choose to cover only some subset of these with radiometers. *LPI/SDA*, however, does not model this case.

2.3.7 FB-ED-BANK/BMW

The Filter Bank–Energy Detect–Bank/Binary Moving Window system is simply a bank of F-ED-BMW systems. As for the FB-ED-T system, simultaneous signal detections in multiple frequency bands are treated as one detection.

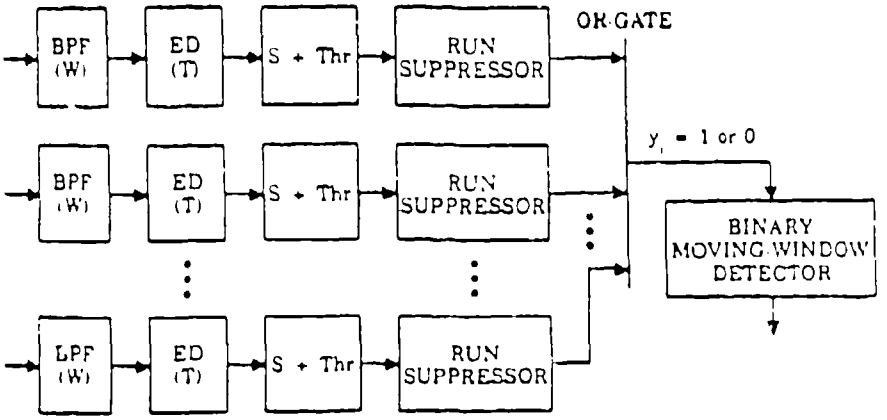

Figure 6: The FB-ED-OR/BMW system. [1]

2.3.8 FB-ED-BMW

The Filter Bank–Energy Detect–Binary Moving Window system performs a moving-window integration of all the binary data, one bit per filter per energy integration interval. This is equivalent to summing the outputs of the binary moving-window integrators in a FB-ED- BANK/BMW system and performing the thresholding operation on that sum.

2.3.9 FB-ED-OR/BMW

The Filter Bank-Energy Detect–OR/Binary Moving Window system, illustrated in Figure 6, uses the knowledge that only one frequency slot is occupied during a particular pulse time by allowing at most a single 1 into the moving-window detector which follows.

2.3.10 FB-ED-OR/C/BMW

Against signals which are both frequency and time hopped, a performance improvement can be realized by using the Filter Bank–Energy Detect-OR/Collapse/Binary Moving Window system, illustrated in Figure 7. The time collapsing function effects a performance improvement in the same manner as it did for the F-ED-C/T system.

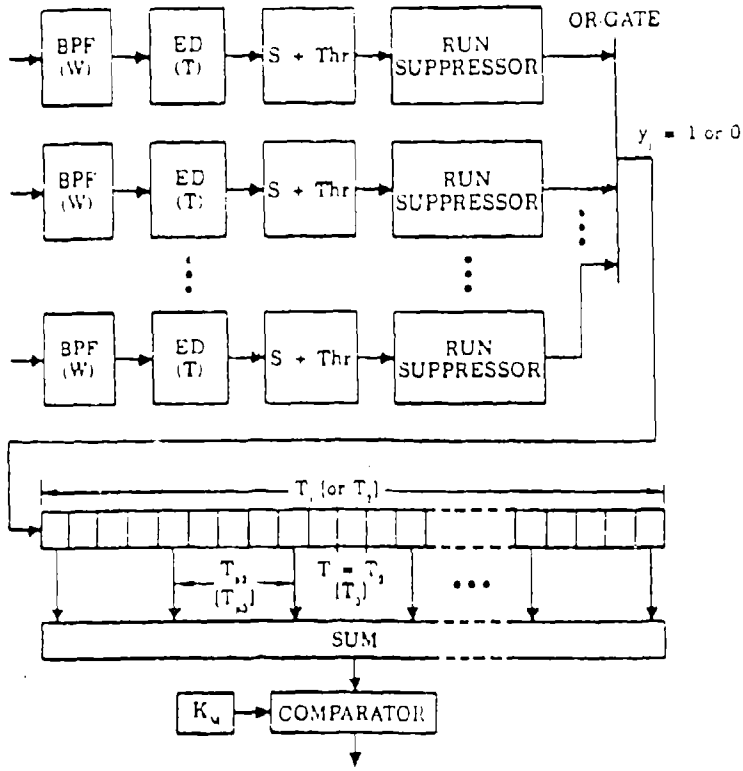

Figure 7: The FB-ED-OR/C/BMW system. [1]

2.3.11 FB-ED-OPT

The Filter Bank–Energy Detect–Optimum system employs a likelihood ratio alarm circuit and is described further in [1].

2.3.12 S-ED-T

The frequency Scanning–Energy Detect–Threshold system, illustrated in Figure 8, is functionally very similar to the fixed single-cell (F-ED-T) radiometer. Whereas the F-ED-T radiometer has a fixed-frequency front-end filter, the S-ED- T system scans the spread bandwidth by using a sweep oscillator to mix the incident signal down to a fixed IF filter. For this particular type of radiometer, the detection of a single pulse is sufficient to cause a message-present decision.

2.3.13 S-ED-BMW

The frequency Scanning–Energy Detect–Binary Moving Window system, illustrated in Figure 9, is the same as the previous system except that the output is fed into a binary moving window detector to reduce the false alarm probability while suffering

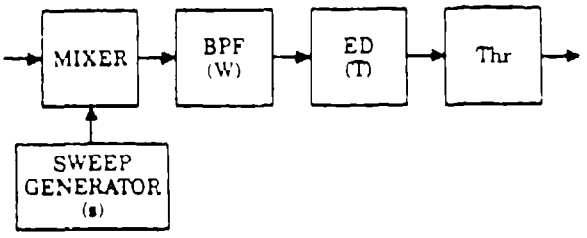

Figure 8: The S-ED-T system. [1]

only minor loss of detection probability. The integration time is assumed to be the signal pulse time.

2.3.14 S/PC-ED-T

The frequency Scanning/Pulse Compression–Energy Detect– Threshold system, illustrated in Figure 10, simply employs a pulse-compression filter, represented by PCF.

2.3.15 S/PC-ED-BMW

The frequency Scanning/Pulse Compression–Energy Detect– Binary Moving Window system, illustrated in Figure 11, simply sends the binary output of the previous system to a binary moving window detector for post-processing.

2.4 Feature Detectors

Feature detection involves signal processing configurations capable of detecting particular parameters or features of spread spectrum waveforms. Although generally less sensitive than radiometers, feature detectors have several advantages that make them extremely powerful tools in detecting, identifying, and parameterizing spread spectrum signals. Primary among these advantages is the ability to measure signal parameters rather than perform only an energy detection function (as the radiometer does). Appropriately designed feature detectors are capable of measuring the chip rate (phase

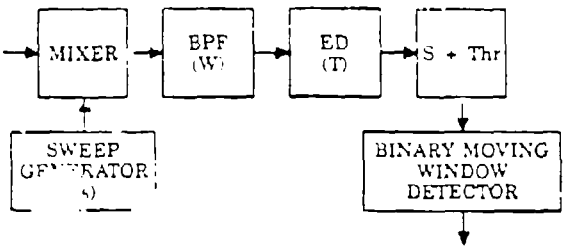

Figure 9: The S-ED-BMW system. [1]

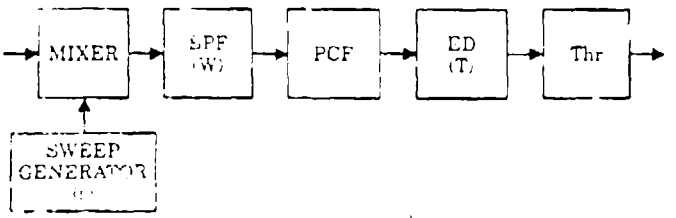

Figure 10: The S-PC-ED-T system. [1]

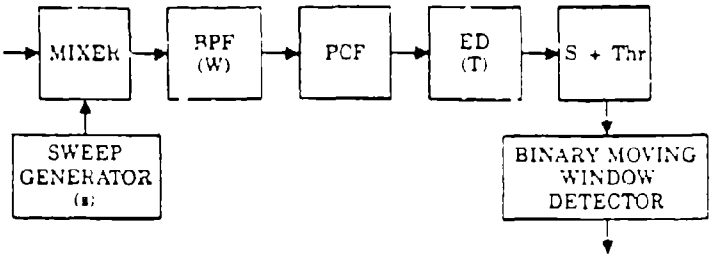

Figure 11: The S/PC-ED-BMW system. [1]

keying rate of the spreading sequence), the frequency-hopping rate, and the time-hop (or pulse) rate of a signal. In general, a feature detector can be conceptually defined to operate against any periodicity (feature) incorporated in the spread spectrum signal.

An additional important advantage is that feature detectors are considerably less susceptible to interference than are pure radiometric detectors. This interference tolerance is largely derived from signal detection away from dc, thus avoiding false signal indications from input power variation. A capability to operate in conjunction with interference can be extremely important in identifying which of a number of signals are of interest or in operating in a cluttered signal environment.

Feature detectors are likely to be an important component of any system designed to detect, identify, and parameterize spread spectrum signals. A number of types of feature detectors which are modelled in *LPI/SDA* are described in the following sections.

2.4.1 Chip Rate Detector (Delay)

One of the most useful, and often the simplest spread spectrum detection device is the chip rate detector. This is a square-law detector that generates a spectral line at the phase keying rate (chip rate). Chip rate lines may be generated for BPSK, QPSK, and SQPSK with varying sensitivities.

The first of two types of chip rate detectors is illustrated in Figure 12. The delay and multiply circuit produces a periodic component (corresponding to the chip rate) and an aperiodic component at the output. The delay is ideally set to half the chip interval, and the filter B is centered at the chip rate, f_c.

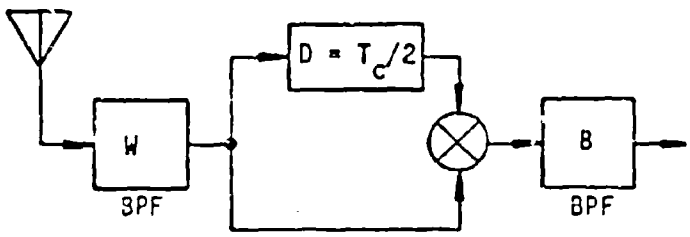

Figure 12: Chip Rate Detector With Delay

2.4.2 Chip Rate Detector (Envelope)

Envelope detection, illustrated in Figure 13, will also generate a chip rate line, especially if τ is set to approximately twice the chip rate. This chip rate detector is especially simple; it differs from a radiometer only by the use of a bandpass filter rather than a lowpass filter (integrator) for detection.

2.4.3 Hop Rate Detector

The hop rate detector, illustrated in Figure 14, generates a spectral line at the hop rate of a frequency-hopped signal. The two front-end filters each cover half of the spread bandwidth of the signal and the squaring operations measure the instantaneous power in each channel. Assuming that the frequency-hopped signal hops into each channel randomly with probability 1/2 (a good assumption) then the output of the differencer is a noisy binary waveform with a periodic component at the hop rate. The remaining operations correspond to a delay-and-multiply chip rate detector as described above to detect the generated spectral line.

2.4.4 Frequency Doubler

The frequency doubler, illustrated in Figure 15, is a feature detector that collapses the spectral spreading of biphase carrier modulation into spectral lines at dc and at twice the original carrier frequency.

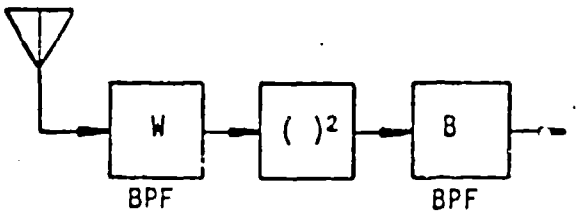

Figure 13: Chip Rate Detector Without Delay

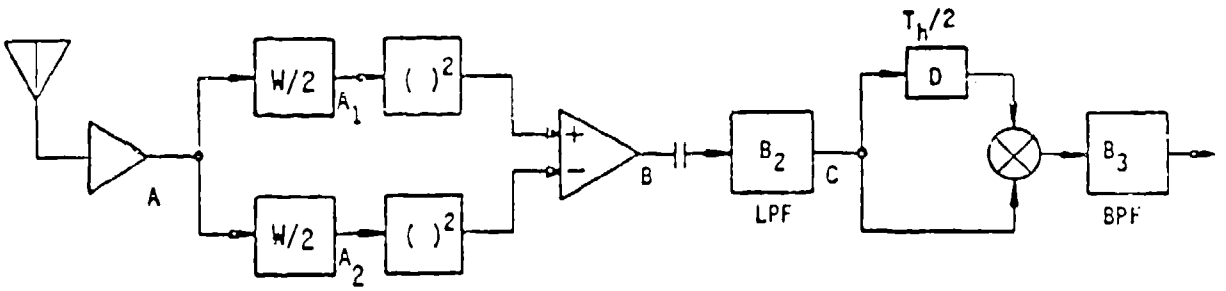

Figure 14: Hop Rate Detector

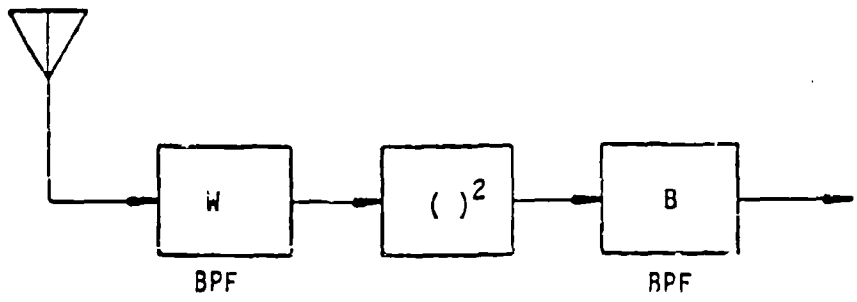

Figure 15: Frequency Doubler

2.4.5 QPSK Quadrupler

For QPSK signals, a quadrupler, illustrated in Figure 16, will generate a feature spectral line at four times the center frequency of the input spectrum.

2.4.6 Time Hop Detector

A time-hopping signal may be viewed as a signal having a frame duration T_0 in which are placed m elements each having duration τ. If element start epochs exist only at integer multiples of τ, and if T is such a multiple, then it is possible to define a time hop detector targeted on the communicator's signal that will generate a spectral line at the element rate, $1/\tau$. Such a detector appears in Figure 17.

2.5 Quality Factors

Gutman and Prescott [2] describe five Quality Factors which act as quantitative measures of the LPI effectiveness in the presence of jammers and intercept receivers. These Quality Factors, which are functions of the communications link parameters and typically expressed in dB, are:

- Antenna Quality Factor $Q_{ant} = G_{tc}G_{et}/G_{ti}G_{it}$ where G_{tc} is the transmitter antenna gain in the direction of the receiver, G_{et} is the receiver antenna gain in the direction of the transmitter, G_{ti} is the transmitter antenna gain in the direction of the interceptor and G_{it} is the interceptor antenna gain in the direction of the transmitter.

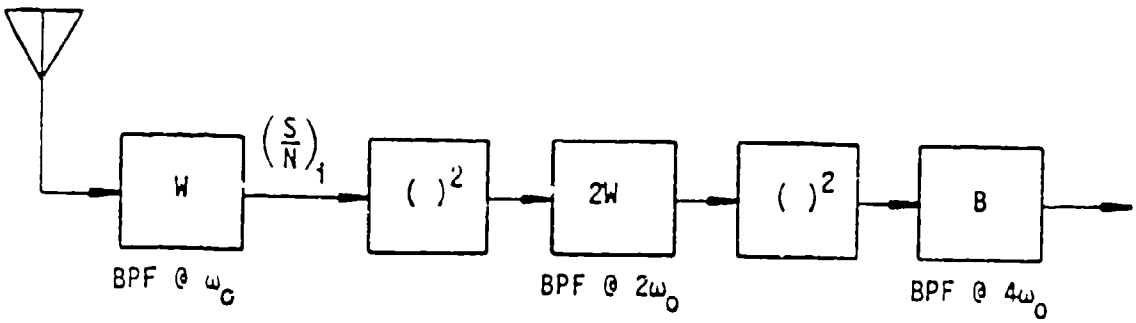

Figure 16: QPSK Quadrupler

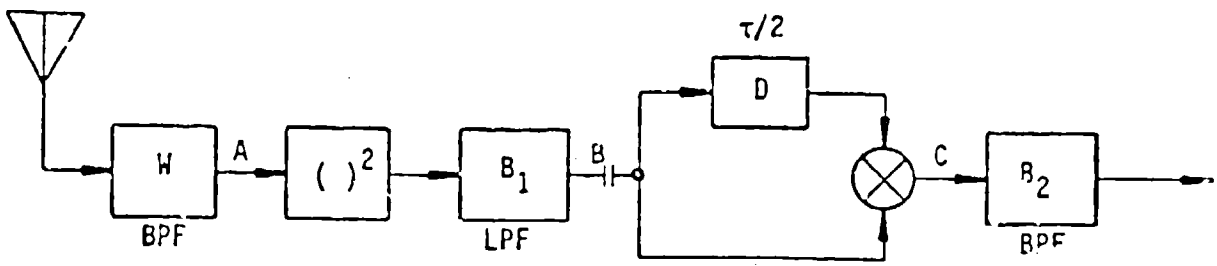

Figure 17: Time Hop Detector

- Atmospheric Quality Factor $Q_{atm} = L_i/L_c$ where L_i and L_c are the losses (other than free space loss) for the interceptor and communications link respectively. These losses include gaseous attenuation, depolarization due to hydrometeors, etc.
- Adaptive Technologies Quality Factor $Q_{ada} = N_i/N_c$ where N_i and N_c are the total received noise powers at the interceptor and receiver respectively. This Quality Factor compares the ability of both the communications and intercept receivers to adaptively filter interference.
- Modulation Quality Factor Q_{mod} – this Quality Factor is the ratio of the signal to noise power spectral densities (SNRs) received at the interceptor and receiver respectively. The SNR at the communications receiver is determined by the tolerable bit error rate, the type of narrow-band modulation used, and the margin required to overcome fading in the channel.
- LPI Quality Factor $Q_{LPI} = (R_c/R_i)^2$ where R_c and R_i are, respectively, the range from transmitter to receiver and from transmitter to interceptor. This Quality Factor is also the product of the other four Quality Factors.

3 Operating Procedures

LPI/SDA allows you to generate four types of results: you can (1) determine the detectability of a particular signal by a certain radiometer, (2) determine the detectability of a particular signal by a certain feature detector, (3) determine the five different Quality Factors associated with the signal, radiometer, and communication link parameters, and (4) plot the Modulation Quality Factor Q_{mod} for a range of one parameter and a family of another. For all of these results, you must describe the signal, the radiometer, and specify a desired probability of detection and probability of false alarm. If you further want to calculate Quality Factors, you must specify certain communication link parameters including narrowband modulation type, probability of bit error, etc. If you then want to generate a plot of Q_{mod} you must select which variables to plot against and their values. The next few subsections describe in detail how to specify a signal and radiometer in *LPI/SDA* and how to enter certain parameters. Section 4, Examples, presents some sample *LPI/SDA* sessions.

3.1 *LPI/SDA* Interface Structure

LPI/SDA contains an inverted tree hierarchical interface. Any page of the interface can be reached from any other, but perhaps not directly, as can be seen in Figure 18, which illustrates the structure of the *LPI/SDA* interface. As you can see in Figure 18, after starting an *LPI/SDA* session you are first presented with the main menu, which

prompts you with the actions which you may take. You can always return to this menu from anywhere in the hierarchy by simply pressing < F1 >, possibly several times if you are deeper than one layer down in the hierarchy.

3.2 Signal Description

Pressing < F2 > when at the main menu (or one level down in the hierarchy) will take you to the Signal Description page. If you have not already chosen a spread spectrum modulation type, *LPI/SDA* will require you to do so before you may do anything else. The up and down arrows will cause each menu item to be highlighted successively, and you should press *Return* to select the spread spectrum modulation type you desire. If you have not already selected a radiometer type (described next), then all of the spread spectrum modulation types in the menu will appear in cyan. If, however, you have previously selected a radiometer type, then some of the spread spectrum modulation types in the menu will appear in gray. The types in gray appear that way because they are not compatible with the radiometer which has been chosen. You may select one of these (presumably with the intent of changing the radiometer type), but no calculations can be performed until the discrepancy is corrected.

After you select a spread spectrum modulation type, a group of signal parameters will appear. The specific group of parameters which appear depends on which modulation type was chosen. The up arrow, down arrow, and carriage return will allow you move the cursor between parameters to specify their value. If the cursor is at the top parameter and you press an up arrow, or it is at the bottom parameter and you press a down arrow or carriage return, then you will again be prompted to select a spread spectrum modulation type. You may select a new one as before, or simply press < Return > to maintain the previous selection.

3.3 Radiometer Description

Pressing < F3 > when you are at the main menu (or one level down in the hierarchy) will take you to the Radiometer Description page. The mechanics of this page are very similar to the Signal Description page. If you have not already specified a radiometer, then you will first be prompted to select a radiometer class, either a single filter or filter bank radiometer system. Next, you will be asked to select a detection model; the detection models are described in section 2.3 and are reviewed in detail in [1]. If you have already selected a spread spectrum modulation type, then some of the detection models may appear in gray if they are not compatible with the chosen modulation type. Here again, you may choose one of the detection models which appear in gray, but you should select another spread spectrum modulation type before attempting to do any calculations.

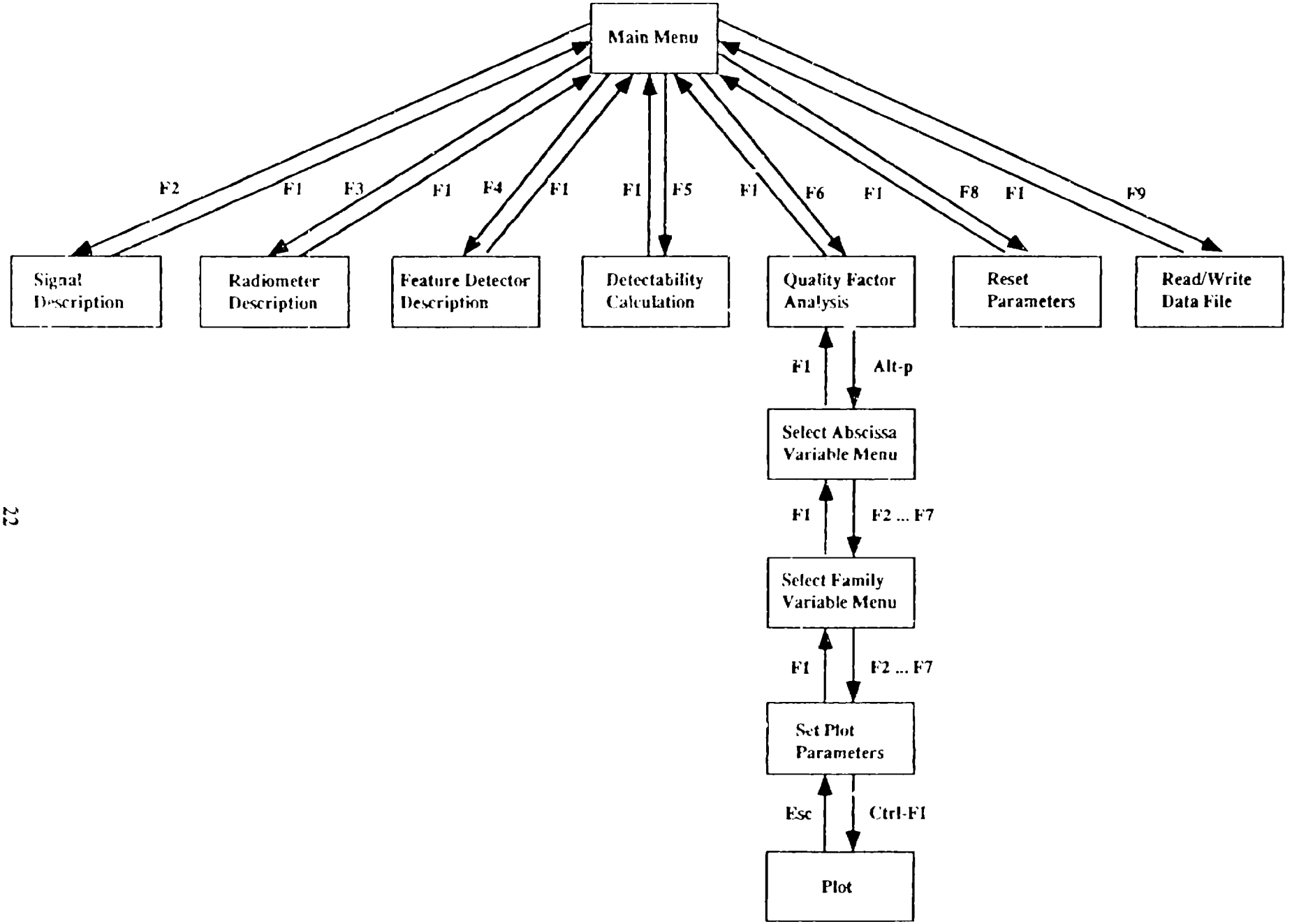

Figure 18: *LPI/SDA* Interface

Some detection models have a single parameter associated with them. If you choose one of these models, then you will be prompted to specify a value for the parameter (a default appears with some of these parameters). After choosing a detection model, regardless of whether it has a parameter associated with it or not, the cursor will appear toward the bottom of the screen. If you want to change the selected detection model, press the up arrow and you will be presented with the detection model menu. To change the radiometer class *and* detection model, press a down arrow when the cursor is at the bottom of the screen.

3.4 Feature Detector Description

Unlike the signal, radiometer, and detectability parameters, a feature detector does not have to be specified in order to perform a detectability calculation. If the feature detector is not completely specified then no detectability information corresponding to the feature detector will be presented on the signal detectability page.

All of the six feature detectors described in section 2.4 are specified in the same manner. First, type < F4 > from the main menu or one level down in the hierarchy. Select one the six feature detector type by using the up and down arrow keys and then < Return >. Next select a narrowband modulation type in the same fashion; and finally, specify a radiometer front end filter bandwidth. When the curser appears in the field for the radiometer front end bandwidth, an up arrow allows the selected narrowband modulation type to be changed and a down arrow allows both the feature detector type and the narrowband modulation type to be changed.

3.5 Reading and Writing Data Files

LPI/SDA has the ability to both read and write data files and clear any data that has already been entered. To clear the data, press < F8 > from either the main menu or from one level down in the hierarchy. All of the user parameters and calculated results will be set to default (unspecified) values.

If some (or all) of the user parameters have been specified and you wish to save these as well as any calculated results, press < F9 > to go to the Read/Write Data File menu. Type 'W' and a prompt will appear asking for the name of the file in which to write the data. If you specify a nonexistent file name, *LPI/SDA* will create a new file with that name; otherwise it will overwrite the existing file with that name. When specifying the file name, *LPI/SDA* will write the file into the current drive and directory unless you specify others explicitly.

Reading a data file is done in a similar manner, except that an 'R' is typed when in the Read/Write Data File menu. If a file name is specified which does not exist or the file cannot be opened, *LPI/SDA* will signal the error. An error will also be signaled if

an attempt is made to read an existing non-*LPI/SDA* data file. To determine whether the data file is of the correct type, *LPI/SDA* opens the file and checks to see if there is a 9876 as the first entry in the file. For data files that were created with versions of *LPI/SDA* before 1.4, the data files will not contain this 9876 marker. To remedy this, simply use any text editor to add the marker to the first line.

3.6 Detectability Calculation

Pressing < F5 > when you are at the main menu (or, again, one level down in the hierarchy) will take you to the Detectability Calculation page. The spread spectrum modulation type, radiometer class, and detection model which you have chosen will appear at the top of the screen. This page requires you to enter two parameters, the probability of detection and the probability of false alarm. Once these parameters are specified, and assuming that you have already specified the signal and radiometer, then pressing < Ctrl-F1 > will cause *LPI/SDA* to calculate the signal detectability. Most calculations should be nearly instantaneous, but some (especially for the binary moving-window systems) might take a few seconds or as much as a few minutes.

3.7 Quality Factor Analysis

After specifying the signal and radiometer and calculating the signal detectability you can, if you choose, calculate the five Quality Factors described in section 2.4 and [2]. Pressing < F6 > when at the main menu (or one level down in the hierarchy) will take you to the Quality Factor Analysis page. Here you will specify a group of link parameters including communications range, intercept range, data rate, probability of bit error, and others. After these are specified, you should press < Ctrl- F1 > to make *LPI/SDA* perform the calculation. The calculated values will appear at the bottom of the screen.

If you wish to see a plot of the Modulation Quality Factor, Q_{mod}, press < Alt-p >. This will take you to the Select Abscissa Variable Menu page. On this page, by pressing the appropriate Function Key, you will choose the variable which you want Q_{mod} to be plotted against. After making this selection, you will then automatically proceed to the Select Family Variable Menu page. *LPI/SDA* allows up to three curves to be generated simultaneously, one for each value of the "family variable." You should choose a family variable in the same manner in which you chose the abscissa variable. Notice, however, that the abscissa variable which you chose appears gray in the Select Family Variable Menu page while the others appear cyan. This is simply because you cannot select the same variable for both the abscissa and family variable.

Now that the abscissa variable and family variable have been chosen, you will advance automatically to the Set Plot Parameters page, the last page you will come to before

actually generating a plot. On this page you must simply specify values for the variable you have selected. For the abscissa variable you must select a minimum and maximum, and for the family variable you must specify at least one and no more than three values. Once these are specified, press < Ctrl-F1 > to start the plot generation. The plot should appear within fifteen to twenty seconds, but may take as long as one minute. After the plot has been generated, press < Esc > to return to the Set Plot Parameters page, and press < F1 > repeatedly to progress back up the hierarchy.

3.8 Errors

LPI/SDA can alert you about four different types of errors: input out of range, parameter(s) unspecified, graphics system failure, and system uncalculable. *LPI/SDA* contains dynamic input range checking on all input parameters. What this really means is that the range which a particular variable must fall in might be a function of others variables which have already been specified. If you specify a value for a variable which falls outside its acceptable range, *LPI/SDA* will alert you with a brief tone and a message which tells you what the current acceptable range for this variable is.

The second type of error, parameter(s) unspecified, occurs when you: (1) try to execute a signal detectability calculation, (2) try to execute a Quality Factors calculation, or (3) try to geuerate a plot before specifying all of the parameters which are required for that calculation. *LPI/SDA* will alert you of this error, but will not tell you which parameter is unspecified.

The third type of error, graphics systems failure,will occur if you attempt to generate a plot and *LPI/SDA* is unable to put the computer in graphics mode because of a nonstandard or improper video adapter.

The final type of error, system uncalculable, might occur for systems which use a binary moving-window detector radiometer. The reason for this is that the mathematics can be intractable for certain combinations of input parameters. Fortunately, the combinations of input parameters which lead to this error are not very practical (e.g., a very large binary moving-window detector threshold k), so you may never encounter this error.

4 Examples

This section will provide you with two examples of using *LPI/SDA* to model the radiometric detection of spread spectrum signals. Both of these examples assume that you are sitting at a computer with *LPI/SDA* on board; they describe the actions to take and the results you should see. The detectability parameters are taken from Woodring and Edell [3] examples 1 and 2. It may be helpful to have Figure 18 handy as you work through these examples.

In the first example we will start the *LPI/SDA* executable, describe a frequency hopped signal, a single filter–energy detect–threshold radiometer, and calculate the required C/N_o to meet the probability of detection and probability of false alarm performance which we will specify.

Make sure that you are in the directory where the *LPI/SDA* executable resides and then type LPISDA. The title page will appear; press any key once to proceed. Now you are at the Main Menu page. You may return to the Main Menu page at any time while working in *LPI/SDA* by typing < F1 >, perhaps repeatedly if you are more than one layer down in the hierarchy; however, if you are familiar with the *LPI/SDA* interface structure it is not necessary to return to this page. The first thing we want to do is describe the signal, so press < F2 >. Now you should be at the Signal Description page, and the cursor should be in the menu to select a spread spectrum modulation type. Press the down arrow once so that frequency hopped is highlighted, and press < Return >. Four parameters should appear in the bottom half of the screen. For the first one, Message Time T_1 (sec), enter 4. For the second, Spread Bandwidth W_1 (Hz), enter 2 GHz, either by typing 2 000 000 000 or 2e9 and then < Return >. Since we are going to be using a single wideband radiometer, it does not matter what the values are of the last two parameters, Number of Frequency Cells N and Number of Pulses b_2, so enter a 1 for each of these.

Now the signal is completely specified, so press < F3 > to proceed to the Radiometer Description page. First you must choose a radiometer class: in this case we want Single Filter Energy Detection, which is already highlighted, so press < Return >. Now you must choose a detection model. Notice that the only detection model which appears in cyan (when it is not highlighted) is Threshold. Recall that this is because no other detection models for this class are compatible with the signal which you specified. Press < Return > to select the Threshold detection model. This model does have a parameter associated with it, Radiometer BW (Hz). The purpose of specifying the radiometer bandwidth is to model the scenario in which either the radiometer does not cover the entire spread spectrum bandwidth, or it covers more than the spread spectrum bandwidth. In this case we want the radiometer to cover the spread spectrum bandwidth exactly, so enter 2 GHz.

You have now specified the radiometer; press < F5 > to proceed to the Detectability Calculation page. Enter 0.1 for the probability of detection and 1e-6 for the probability of false alarm. Now you are ready to calculate the required C/N_o. Press < Ctrl-F1 >, and *LPI/SDA* should calculate a required C/N_o of 48.9 dB-Hz, which agrees perfectly with example 1 in [3].

For the second example, we will determine the detectability of a single hop of the frequency hopped signal, and then calculate the Quality Factors associated with a particular link geometry. Finally, we will generate a plot of Q_{mod} versus probability of detection for a family of three integration time values.

Press < F2 > to return to the Signal Description page. Change the message time to 5e-4 seconds, and the spread bandwidth to 2000 Hz. Proceed to the Radiometer Description page by typing < F3 > and change the radiometer bandwidth to 2000 Hz. Press < F5 > to go to the signal detectability page and calculate the required C/N_o once again by tying < Ctrl-F1 >. The calculated value should be 41.74 dB-Hz, which is very nearly the 41.7 dB-Hz reported in [3].

Now press < F6 > to go to the Quality Factor Analysis page. Select QPSK as the narrowband modulation type. Enter 1e-5 for Pe (probability of bit error), 4 dB for the comm link margin, 0 for L_i/L_c (the ratio of path losses other than free space losses for the intercept and communications link), 1 Mbps for the data rate, 16 dB for $G_{tc} + G_{cr}$ (the sum of the transmitter antenna gain in the direction of the receiver and the receiver antenna gain in the direction of the transmitter), 9 dB for $G_{ti} + G_{ri}$ (the sum of the transmitter antenna gain in the direction of the interceptor and the interceptor antenna gain in the direction of the transmitter), 260 k for T_{oc} (the noise temperature of the receiver in Kelvins), and 270 k for T_{oi} (the noise temperature of the interceptor). Press < Ctrl-F1 > to calculate the five Quality Factors. Now press < Alt-p > to proceed to the Select Abscissa Variable Menu page. Press < F2 > to select probability of detection as the variable to plot against. After making this selection you will automatically proceed to the Select Family Variable Menu page. Press < F4 > to select radiometer integration time as the family variable; you will now proceed automatically to the Set Plot Parameters page. Enter 0.05 for the lower bound of P_d (the probability of detection), 0.95 for the upper bound, and enter 3e-4, 5e-4, and 7e-4 respectively for the three family values of the radiometer integration time. Now press < Ctrl-F1 > to generate the plot, and press < Esc > when you are finished viewing the plot.

These examples have demonstrated basically all of the things which you may do in *LPI/SDA*. With only a very little bit of experience you should acquire expertise in using *LPI/SDA*'s simple user interface.

References

[1] Dillard, George M. and Robin A., "Detectability of Spread-Spectrum Signals," Artech House, Norwood, MA, 1989.

[2] Gutman, Lawrence L. and Prescott, Glenn E., "System Quality Factors for LPI Communications".

[3] Woodring, D. and Edell, J., "Detectability Calculation Techniques," U.S. Naval Research Laboratory, Code 5480, Sept. 1, 1977.